Acta Geochim (2024) 43:214–234
https://doi.org/10.1007/s11631-023-00651-5

ORIGINAL ARTICLE

Weathering and accumulation of trace elements in the soils of the Porali Plain, Balochistan: repercussions in agriculture

Maria Kaleem[1] · Erum Bashir[1] · Shahid Naseem[1] · Tahir Rafique[2] · Bushra Shahab[1]

Received: 17 April 2023 / Revised: 17 August 2023 / Accepted: 30 October 2023 / Published online: 24 November 2023

Abstract This study is the first attempt to assess the nature of the soil, especially on the western side of the Porali Plain in Balochistan; a new emerging agriculture hub, using weathering and pollution indices supplemented by multivariate analysis based on geochemical data. The outcomes of this study are expected to help farmers in soil management and selecting suitable crops for the region. Twenty-five soil samples were collected, mainly from the arable land of the Porali Plain. After drying and coning-quartering, soil samples were analyzed for major and trace elements using the XRF technique; sieving and hydrometric methods were employed for granulometric analysis. Estimated data were analyzed using Excel, SPSS, and Surfer software to calculate various indices, correlation matrix, and spatial distribution. The granulometric analysis showed that 76% of the samples belonged to loam types of soil, 12% to sand type, and 8% to silt type. Weathering indices: CIA, CIW, PIA, PWI, WIP, CIX, and ICV were calculated to infer the level of alteration. These indices reflect moderate to intense weathering; supported by K_2O/Al_2O_3, Rb/K_2O, Rb/Ti, and Rb/Sr ratios. Assessment of the geo-accumulation and Nemerow Pollution indices pinpoint relatively high concentrations of Pb, Ni, and Cr concentration in the soils. The correlation matrix and Principal Component Analysis show that the soil in this study area is mainly derived from the weathering of igneous rocks of Bela Ophiolite (Cretaceous age) and Jurassic sedimentary rocks of Mor Range having SEDEX/MVT type mineralization. Weathering may result in the undesirable accumulation of certain trace elements which adversely affects crops.

Keywords Weathering indices · Pollution indices · Accumulation · Repercussions · Trace elements · Multivariate analyses · Porali Plain · Balochistan

✉ Maria Kaleem
maaria_kaleem@yahoo.com

[1] Department of Geology, University of Karachi, Karachi 75270, Pakistan

[2] Applied Chemistry Research Centre, PCSIR Laboratories Complex, Karachi 75280, Pakistan

1 Introduction

Soil is a non-renewable weathering product of rocks, generated by the prolonged pedogenesis process (Wani et al. 2022). In the study area, sedimentary and igneous rocks are exposed, which upon physical and chemical weathering gradually convert into soil (Sirbu-Radasanu et al. 2022), influenced by the parent rock composition and related environmental fate (Shaltami and Bustany 2021). In the recent past, academia and public sector agriculture organizations started paying attention to appraise the impact of some toxic elements (Cr, Pb, Cd, etc.) on agricultural soil and crop growth (Mao et al. 2023). Evaluation of weathering indices is important to assess soil fertility, soil erosion, rock weathering, and availability of essential nutrients derived from rock weathering which affects agriculture and can have environmental consequences (Hasan et al. 2023). The pertaining elements are dispersed in the soil and are available for crops to uptake. During weathering, feldspars are easily chemically altered, resulting in the depletion of alkalis; sodium (Na),potassium(K), and alkaline earth elements; calcium (Ca), with preferential enrichment of Al_2O_3 (Heidari et al. 2022). Parameters used to assess the degree of weathering and alteration (Deng et al. 2022; Pandarinath 2022), such as the Chemical Index of Alteration (CIA), Chemical Index of Weathering (CIW), Plagioclase Index of Alteration (PIA), Product of Weathering Index (PWI), Weathering Index of Parker (WIP), Modified Chemical Index of Alteration (CIX), Index of Compositional Variability (ICV) and Ruxton Ratio (RR) (Fiantis et al. 2010). Elemental ratios of K_2O/AI_2O_3 and Rb-type Indices (Rb/K_2O, Rb/Ti, and Rb/Sr ratios) are also significant in this context (Perri 2020; Négrela et al. 2018). These indices are valuable to infer the extent of weathering, during the soil formation process (Gonçalves et al. 2022). The geo-accumulation Index and the Improved Nemerow Index are two significant assessment methods to attain better environmental health management (Zhao et al. 2021; Gao et al. 2021). These indices are assessed from the geochemical background, to discriminate the natural quantity of a given constituent in the environment from the extent originated because of human activity (Gonçalves et al. 2022; Kazapoe and Arhin 2021). The rapid urban population growth and industrialization may contaminate the agricultural soil with several toxic elements (El-Anwar et al. 2019). Accumulation of certain trace elements in the soil creates some adverse effects on the crops. A few of them are listed in Table 1.

Lasbela is one of the most fertile and productive districts of Balochistan with the majority of the local population engaged in agriculture. The total cultivated area of the district is 81,275 hectares and a further 895,271 hectares of land has the potential for agricultural usage (SMEDA 2022). At present, the Government of Balochistan itself is working to improve the provincial production rate. Areas around the western side of the Porali Plain and the foothill of the Haro Range are new extended land in the agricultural zone of the region. The present study is an initial effort on the soil of the new emerging agriculture hub to provide a more comprehensive assessment of weathering intensity to specify the nature of the soil and the degree of accumulation of trace elements in the soil resulting from weathering to a better representation to weathering patterns and provide insights into the weathering processes operated in an area to achieve its suitability for agriculture. This study is also aimed to discuss the biological role of Pb, Ni, Cr, and Sr, and their related adverse impacts on some of the sensitive crops of the study area based on available literature. The outcome of the present work will help farmers with better yields and adopt preventive measures.

2 Materials and methods

2.1 Sampling technique

Following the removal of surplus surface material/contamination, 25 composite soil samples were collected randomly from different areas of the Porali Plain, District Lasbela, Balochistan (by digging small pits of 30 cm depth using a hand auger) along both sides of Karachi-Quetta N-25 Highway (Table 2 and Fig. 1). Most samples were taken from arable land having mature soil profiles; however, a few samples (JS, GC, JD and KN) were collected from the cultivated land situated next to the outcrops of rocks of Ferozabad Group and BelaOphiolite. Samples were appropriately stored and labelled for transportation from the collection site to the lab.

Table 1 Biological role of Pb, Ni, Cr and Sr, their adverse effects and list of sensitive crops

Element	Biological role	Adverse impact	Sensitive crops	Significant References
Pb	It is a non-essential and considered toxic element, even at trace concentrations	Pb hinders photosynthetic activity, causing chlorosis. It also interferes functions of enzymes	Soybean, wheat, spinach, cabbageand peas	Osman and Fadhlallah, (2023), Mao et al. (2023), Collin et al. (2022)
Ni	Trace amount of Ni is considered a vital micro-nutrient, required by the crops for proper metabolic functions	High Ni in the soil upset the nitrogen metabolism, causing slow growth and germination	Wheat, bitter ground, rice, maize and sweet potato	Khan et al. (2023), Mustafa et al. (2023), Kumar et al. (2022)
Cr	Beneficial biological role of Cr has so far not been found in literature	Cr shunted the plant growth, chlorosis in leaves, alter enzymatic activities, less yield	Beans, sunflowe Wheat, pea, rice, maize, bean, and barley	AbdElgawad et al. (2023), Ali et al. (2023), Wani et al. (2022)
Sr	The function of alone Sr^2 is not clear, however it has analogous behavior as Ca^{2+} in the plant, required for healthy growth	High intake of Sr ions was often associated with decreased chlorophyll	Wheat, rice, barley,cabbage, silver poplar, red fescue, red clover	Srikhumsuk et al. 2023, Liang et al. (2023), Zhang et al. (2020a, b)

Table 2 Major composition of the soils of Porali Plain (wt%), Lasbela, Balochistan

Area of study	S.#	SiO_2	TiO_2	Al_2O_3	Fe_2O_3	MnO	MgO	CaO	Na_2O	K_2O	P_2O_5
Gacheri	GC	53.49	0.85	12.58	5.87	0.23	2.93	12.09	0.98	1.65	0.17
RohriDhora	RD	48.77	1.34	11.87	8.76	0.39	3.86	12.73	0.79	0.82	0.21
JandroDhora	JD	42.76	0.71	11.70	4.69	0.22	1.77	20.24	0.67	1.60	0.15
Wayaro North	WN	49.94	1.09	12.54	7.9	0.28	6.35	11.41	1.14	1.03	0.22
GajriNai	GN	52.98	0.75	13.40	5.98	0.24	4.24	11.43	1.04	1.30	0.18
Muka	MK	50.94	0.81	13.69	4.66	0.19	2.56	14.06	1.08	1.18	0.17
Titan Dhora	TD	57.17	0.74	11.98	6.21	0.17	4.13	9.54	0.93	1.43	0.21
KhuniDhora	KD	49.43	0.71	12.84	5.08	0.21	4.22	13.59	1.35	1.53	0.17
Qaiser Goth	QG	49.54	0.58	12.93	4.18	0.15	2.46	15.21	0.92	1.48	0.21
Chankara	CH	60.23	0.69	10.42	5.01	0.17	4.33	9.47	1.03	1.02	0.23
Sadoori	SA	52.37	0.88	11.76	5.52	0.17	3.61	12.98	1.15	1.04	0.17
Jarka	JK	50.37	0.65	13.72	5.62	0.16	2.68	13.88	1.22	1.28	0.14
JhalJhao	JJ	63.62	0.84	10.45	3.57	0.16	2.12	9.43	1.31	0.95	0.13
Abu Goth	AG	56.74	0.64	12.18	4.79	0.17	3.09	11.24	1.12	1.32	0.17
Sadrani	SR	52.76	0.97	11.82	5.82	0.22	4.02	12.53	0.97	1.14	0.18
Mullaka	ML	50.78	0.77	10.22	5.33	0.23	3.64	14.91	0.95	1.41	0.11
Chib Ammo	CA	57.62	0.93	10.65	5.73	0.21	3.25	10.65	1.35	1.24	0.11
Kanar	KN	50.29	0.55	12.78	4.12	0.18	2.31	14.85	0.88	1.36	0.21
JuskaShahuk	JS	52.89	0.91	13.51	6.05	0.24	4.54	11.03	1.27	0.98	0.19
Tethyn	TH	52.26	0.64	12.24	4.92	0.19	3.18	13.23	1.51	1.01	0.17
Dhak	DK	47.72	0.79	12.01	5.37	0.16	3.19	15.75	0.85	1.66	0.15
Haro	HA	54.91	0.32	10.43	3.18	0.32	1.60	15.73	0.65	0.76	0.14
PirBambal	PB	55.88	0.55	12.32	4.91	0.24	2.25	12.18	0.86	0.89	0.16
MianiHor	MH	45.91	0.48	13.42	3.77	0.16	2.97	16.98	0.83	0.99	0.16
Luna Dhora	LD	55.11	0.64	12.58	5.03	0.17	2.76	12.02	1.22	1.13	0.15
Mean		52.58	0.75	12.16	5.22	0.21	3.28	13.09	1.04	1.21	0.17
Minimum		42.76	0.32	10.22	3.18	0.15	1.60	9.43	0.65	0.76	0.11
Maximum		63.62	1.34	13.72	8.76	0.39	6.35	20.24	1.51	1.66	0.23
Median		52.37	0.74	12.24	5.08	0.19	3.18	12.73	1.03	1.18	0.17
RSD (%)		1.27	0.59	1.87	0.14	3.03	2.53	1.61	3.67	4.04	3.70

2.2 Sample processing and analysis

The soil was dried at room temperature in an aerated place for a few days, following which a portion of raw soil samples was used for grain size analysis: using sieving, hydrometric method, and sedimentograph respectively. For the estimation of chemical constituents, samples were reduced in quantity by coning and quartering method and sieved through a 200-mesh polyethylene screen. A small amount ($\sim$ 25 g) was dried at 105 °C in an electric oven and stored in an air-tight plastic jar. Major and trace elements of soil samples were analyzed employing an advanced X-ray fluorescence (XRF) technique, using a Thermo Fisher Scientific Niton XRF analyzer. It is an easy, rapid, and handy technique that was used in the present study to evaluate trace element concentrations in soil (Declercq et al. 2019; Hu et al. 2017). Sieved (200 mesh) samples were placed in an X-ray sample cup covered with a 4.0-µm prolene X-ray film. The measurement time for all the measurements was 120 s. The instrument was set at All Geo Mode which automatically estimates elemental composition. The quality of sample analysis was controlled by randomly introducing and analyzing standard soil reference samples (NIST 2709a PP and RCR A PP), to perform the most accurate calibration and to check the competence of the laboratory.

The handheld XRF can excite low ($Z < 18$) atomic number elements (Laperche and Lemière 2021), leading to unreliable results. To avoid this issue, Na was estimated through flame photometry. Pulverized (-200 Mesh) 100 mg soil sample was digested using a mixture of hydrofluoric acid (HF) and perchloric acid ($HClO_4$) in a 100 mL Teflon beaker (Bankaji et al. 2023). Stock standard solutions of Na (1000 mg/L) were diluted, using ultra-high purity water, with 3, 5, 7, 9, 12, and 15 mg/L concentrations of Na. These standard solutions of Na were aspirated and the

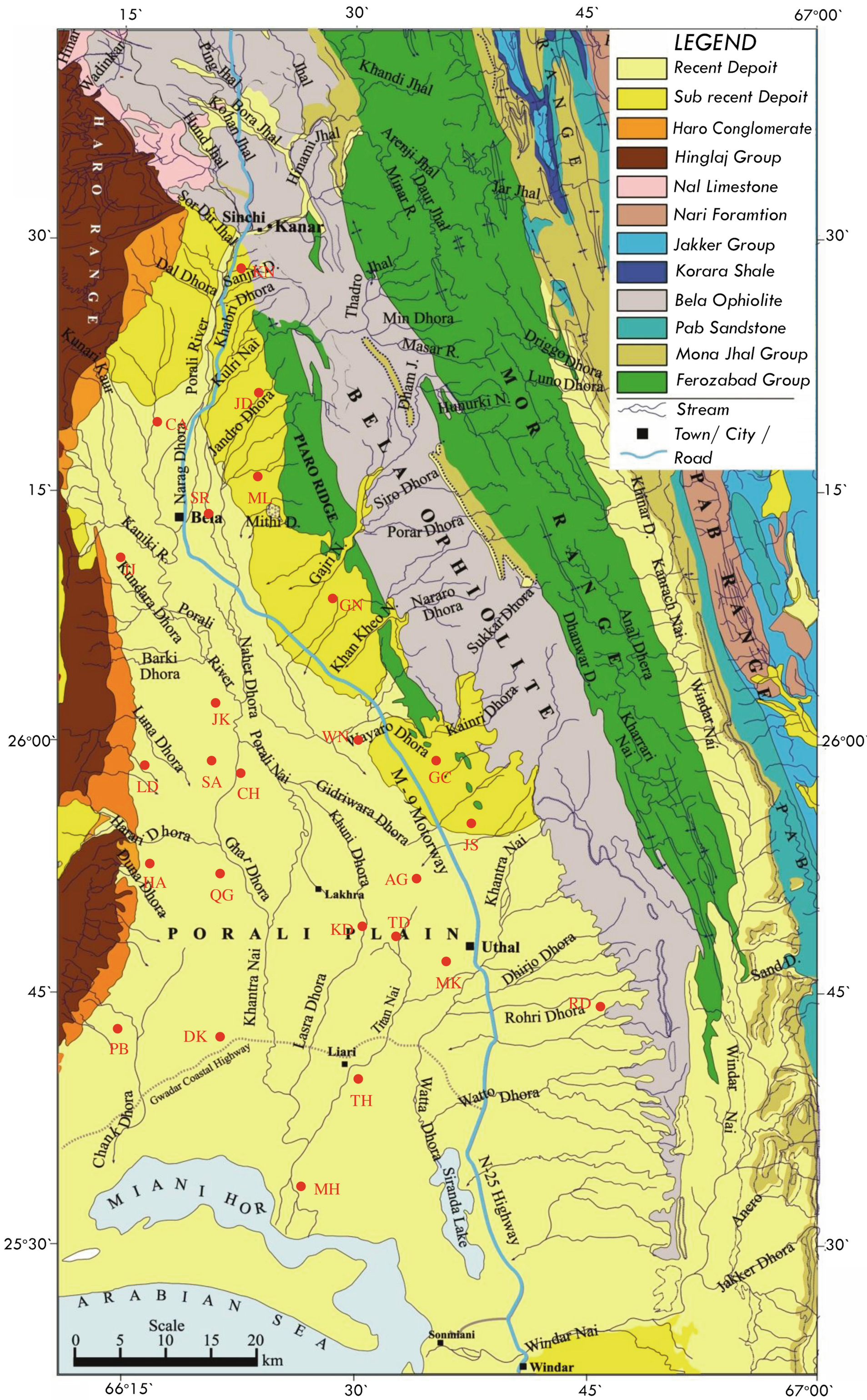

Fig. 1 Geological map of the study area showing sites of soil samples (red spot) (Simplified after HSC 1960)

resulting emission intensities of light were noted. Working curves were prepared, by plotting intensity against concentration, to compute the amount of Na_2O in the soil (Wei et al. 2023).

Precision and accuracy of analytical data are crucial for a quality research paper. In general, erroneous analytical results are more common in the case of gravimetric and volumetric analysis, however, their occurrence is minimized in the case of instrumental analysis. The X-ray fluorescence (XRF) method is a sophisticated analytical technique that needs no digestion and dilution so that XRF analytical data is relatively precise and accurate (Sabouanget al. 2023; Sultana et al. 2023). Despite the fact, that relative standard deviation (RSD) is a routine application to verify the authenticity of the analytical data. For this purpose, it is recommended to analyze samples in duplicate, to obtain a repeatable and reproducible result.

The RSD can be assessed, using a coefficient of variation and expressed as a percentage:

$$\%\ \mathrm{RSD} = s/\bar{x} \times 100$$

Where s = standard deviation, $\bar{x}$ = arithmetic mean.

The RSD of all major oxides was computed, it ranges from 0.14 to 4.04 (Table 2), showing an acceptable reliable procedure. The RSD noted relatively high in the case of K_2O (4.04%), P_2O_5 (3.70%), Na_2O (3.67%), moderate MgO (2.53%), Al_2O_3 (1.87%), CaO (1.61%) and SiO_2 (1.27%), while rest have comparatively low (< 1.0%) RSD values (Table 2). An RSD value < 4.7%, indicates a good result (Nadporozhskaya et al. 2022).

2.3 Computation of indices and other multivariate parameters

Estimated analytical data was processed for the calculation of various statistical parameters, weathering, pollution, and accumulation indices to explicate the repercussions of elements in soil for agricultural use.

Nesbitt and Young (1982) introduced a simple expression to evaluate the degree of weathering in an area, with exposed igneous rocks. The Chemical Index of Alteration is based on the molar ratio of mobile elements (Na_2O, K_2O, and CaO*) and immobile elements (Al_2O_3 and Fe_2O_3) representing the weathering of feldspars.

$$\mathrm{CIA} = (Al_2O_3)/[Al_2O_3 + Na_2O + K_2O + CaO*] \times 100 \quad (1)$$

Per the CIA index categorization, values < 50, indicate very poor weathering, value up to 60 specifies weak, and values between 60 and 80 represents moderate, and exceeding 80 represents a strong-stage weathering zone.

The Chemical Index of Weathering is calculated using the following equation.

$$\mathrm{CIW} = (Al_2O_3)/[Al_2O_3 + Na_2O + CaO*] \times 100 \quad (2)$$

In addition to CIA, the Plagioclase Index of Alteration (PIA) is another significant index to appraise the degree of weathering, particularly plagioclase feldspars (Sirbu-Radasanu et al. 2022). The PIA can be measured from the following equation (Fedo et al. 1995):

$$\mathrm{PIA} = (Al_2O_3 - K_2O)/[Al_2O_3 + Na_2O + CaO * - K_2O] \times 100 \quad (3)$$

Souriet al. (2006) presented a modified chemical index known as the Product of Weathering Index (PWI), considering the mole ratio of SiO_2 with combined oxides of TiO_2, Fe_2O_3, SiO_2, and Al_2O_3.

$$\mathrm{PWI} = [SiO_2/(TiO_2 + Fe_2O_3 + SiO_2 + Al_2O_3)] \times 100 \quad (4)$$

The Weathering Index of Parker (WIP) is calculated by using the molar amount of alkaline (Na_2O and K_2O), and alkaline earth oxide (CaO and MgO) and eliminated Al_2O_3, as follows (Deng et al. 2022).

$$\mathrm{WIP} = [2Na_2O/0.35] + [2K_2O/0.25] + [CaO/0.7] + [MgO/0.9] \times 100 \quad (5)$$

To avoid the impact of high Ca from carbonate rocks, Garzanti et al. (2014) modified the CIA developed by Nesbitt and Young (1982), and introduced a simple expression, by eliminating moles of CaO, which was not derived from the igneous rocks:

$$\mathrm{CIX} = (Al_2O_3)/[Al_2O_3 + Na_2O + K_2O] \times 100 \quad (6)$$

Cox et al. (1995) presented an index of compositional maturity of the alumino-silicates, based on the mole proportion of several oxides simultaneously as shown in the following expression.

$$\mathrm{ICV} = [(Fe_2O_3 + K_2O + Na_2O + CaO + MgO + MnO + TiO_2)]/(A1_2O_3) \quad (7)$$

Müller (1969) was the first to introduce the term geo-accumulation Index or I_{geo} for qualitative assessment of heavy metal pollution in soil. To appraise the trace element pollution, the equation for I-geo is:

$$I_{geo} = \mathrm{Log}_2 C_n/1.5B_n \quad (8)$$

where: C_n is the concentration of trace elements in the soil, B_n is the geochemical background concentration of the trace element (Bhuiyan et al. 2021), and the constant of 1.5 in the equation is to lessen the influence of any variations (Wang et al. 2019).

The Nemerow Pollution Index (I_N) highlights the influence of the highest concentration of pollutants. The traditional Nemerow index was improved by replacing the single-factor index with I_{geo}. The following equation was developed:

$$\mathrm{IN} = \sqrt{I_{geomax}{}^2 + I_{geoave}{}^2/2} \quad (9)$$

where I_N is the comprehensive picture of the contamination index of the study area, I_{geomax} is the maximum I_{geo} value of such sample, and I_{geoave} is the arithmetic mean value of I_{geo}.

Correlation matrix and multivariate analyses were done using the SPSS software and spatial distribution patterns of indices and other parameters were generated with the help of the Golden Surfer software.

3 Study area's general geology

The study area represents the western part of the Indian Plate and is bounded by the Ornach-Nal Fault in the west and the Porali Plain in the south (Bykov and Merkulova 2022). Geologically, the study area is located in the Porali Plain, surrounded by the Haro Range in the west, the Mor Range in the east, and the Miani Hor in the south (Syed et al. 2020). The Porali Plain is a triangular-shaped, lowland area occupied by recent to sub-recent soil cover and alluvium deposits (Siddiqui and Jadoon 2013). Sedimentary rocks of the Jurassic along with igneous rocks of Bela Ophiolite (Cretaceous) are widely exposed in Mor Range (Kaleem et al. 2021). The sedimentary rocks of Mor Range contain significant deposits of barite, zinc, lead, iron, and copper (Arain et al. 2021). Bela Ophiolite (BO) of Cretaceous age is related to Neotethyan Supra-subduction Zone (SSZ) ophiolites formed due to the rapid convergence of India with Eurasia and faced multiple subduction phases (Jalil et al. 2023; Bhat et al. 2021). Exotic blocks of variable segments of BO are found in an N-S striking belt between the sedimentary rocks of the Mor Range. Medium to small-sized metallic mineral deposits (Mn, Fe, Cr, Cu, etc.) are also associated with the different segments of BO in the study area (Rashid et al. 2022). The western mountainous range is termed as Haro Range, mainly consisting of the Nal Limestone of Oligocene, Hinglaj Formation of Pliocene, and Haro conglomerate of Pleistocene age.

4 Results and discussion

4.1 Soil granulometry

Soil granulometry is used to understand the soil formation processes, operative in an area (da Silva et al. 2022). Soil texture gives an idea about soil's aeration, water- and nutrient-holding capacities (Ahmadi et al. 2021) and helps select suitable crops for harvesting to obtain a good yield (Barman and Choudhury 2019). Soil texture refers to relative quantities of clay, silt, and sand; presented on a ternary diagram (Shamkhi and Al-Badry. 2022). According to Martín et al.'s (2018) sand-silt–clay ternary diagram, 28% of the samples studied were silt loam, followed by 24.0% sandy loam, 16% loam, 12% sand, and 8% silt. Loamy sand, silty clay loam, and clay type each represented one sample (Fig. 2). Of the 25 samples studied, 19 were spread in the zones of loam soils. These soils are rich in nutrients and minerals, having good water holding capacity with draining excessive water and providing loose spaces for the spreading and growing of roots. Loamy soils are easier for farmers to cultivate and are suitable for the growth of wheat, oil seeds, tomatoes, onion, maize, green beans, and okra; these medium-textured soils are frequently thought of as perfect for agriculture (Parikh and James 2012).

4.2 Chemical composition

4.2.1 Major elements

The major elemental composition, in the form of oxides of the soils of the Porali Plain, is summarized in Table 2, with basic statistics. The mean abundance displays SiO_2 (52.58%) as one of the principal elements, followed by CaO (13.09%), Al_2O_3 (12.16%), Fe_2O_3 (5.22%), MgO (3.28%), K_2O (1.21%), Na_2O (1.04%), while TiO_2 (0.75%), MnO (0.21%) and P_2O_5 (0.17%) were noted low (Table 2).

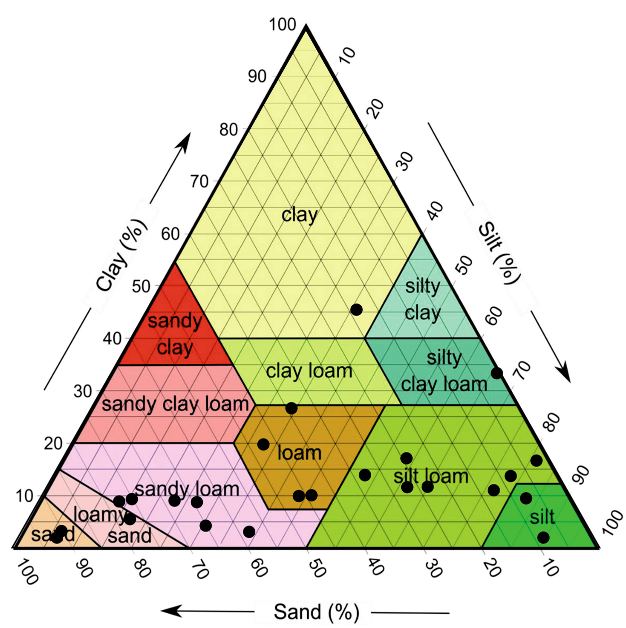

Fig. 2 Soil texture of study area, on (sand–silt–clay) ternary diagram (fields are after Shamkhi and Al-Badry 2022)

4.2.2 Trace elements

Eleven trace elements were detected by the XRF (Table 3), among them; Ti (av. 3932 mg/kg) had the highest concentration, followed by Mn (av. 1620), Ba (av. 298), Sr (av. 245), Cr (av. 184), V (av. 142), Ni (av. 79), Zn (av. 69), Pb (av. 65), Cu (av. 43) and Rb (av. 26). During the weathering process, these trace elements are leached out and concentrated in the soil. Some (Mn, Zn, Cu, and Ni) are essential micronutrients, while Pb, Ni, and Cr are moderately poisonous. The mean amount of certain trace elements (Cu, Ni, Cr, V, Mn, Pb, Ba, and Rb) in the studied soil samples is higher than the average amount of the world soils, as suggested by Alloway (2005), and Kabata-Pendias and Pendias (2001). The amount of Ti, Zn, and Sr in the studied soil samples is nearly close to the world average (Fig. 3).

4.3 Role of chemical weathering on soil

The application of various weathering indices is important to outline the type of weathering process and pedogenesis, operative in an area (Pandarinath 2022). Major oxides of the soils are estimated (Table 2) and converted into mole fractions, by dividing the respective molecular weight of the oxides. In general, all indices are based on the mole ratio of immobile oxides (Al_2O_3, Fe_2O_3, and TiO_2) and the mobile fraction of feldspars, mainly Na_2O, K_2O, CaO, and

Table 3 Trace elements data of the soils of Porali Plain, Lasbela, Balochistan (values are in mg/kg)

Area of study	S.#	Cu	Ni	Cr	V	Ti	Mn	Pb	Zn	Ba	Sr	Rb
Gacheri	GC	55	90	178	157	3968	1781	40	68	439	237	33
RohriDhora	RD	88	76	214	225	6235	3021	48	73	210	199	10
JandroDhora	JD	49	43	129	103	2903	1704	63	90	605	351	36
Wayaro North	WN	82	134	252	206	5991	2169	68	71	350	248	18
GajriNai	GN	53	75	177	159	4070	1859	184	134	207	187	24
Muka	MK	39	59	144	123	3432	1472	28	55	415	311	23
Titan Dhora	TD	53	47	158	172	4469	1317	51	82	275	279	39
KhuniDhora	KD	43	45	185	155	4270	1626	14	70	198	227	30
Qaiser Goth	QG	29	54	194	137	3524	1162	342	56	235	188	29
Chankara	CH	33	113	133	132	4180	1317	17	72	228	254	31
Sadoori	SA	35	79	182	127	3737	1317	201	119	302	246	31
Jarka	JK	51	81	185	126	3664	1239	42	60	236	205	28
JhalJhao	JJ	32	50	182	121	3198	1239	275	47	233	247	19
Abu Goth	AG	45	58	176	145	4048	1317	21	63	259	192	26
Sadrani	SR	45	98	161	157	4767	1704	14	63	490	266	22
Mullaka	ML	47	107	196	161	4703	1781	38	70	351	215	25
Chib Ammo	CA	39	131	200	145	4372	1626	19	76	278	229	28
Kanar	KN	36	71	143	109	3023	1394	23	60	485	286	28
JuskaShahuk	JS	54	143	253	163	4556	1859	27	70	355	228	16
Tethyn	TH	43	89	171	138	3749	1472	21	55	221	245	28
Dhak	DK	29	45	180	160	4259	1239	16	69	245	218	33
Haro	HA	26	81	158	84	1752	2478	22	45	296	322	16
PirBambal	PB	30	63	286	108	3006	1859	17	48	242	229	20
MianiHor	MH	25	61	208	99	2547	1239	24	43	135	321	19
Luna Dhora	LD	35	71	162	153	3883	1317	17	64	168	208	33
Mean		43.84	79	184.3	142.6	3932	1620	65.3	68.9	298.3	245.5	25.8
Minimum		25	43	129	84	1752	1162	14	43	135	187	10
Maximum		88	143	286	225	6235	3021	342	134	605	351	39
Median		43	75	180	145	3968	1472	27	68	259	237	28
Average soil †		20*	20	54	58	3500	437*	32	64*	45	210	50
Background values !		38.9	29	59.5	129	60	–	27	70	460	175	68

*Alloway (2005)

†Kabata-Pendias and Pendias (2001)

!Kabata-Pendias (2011)

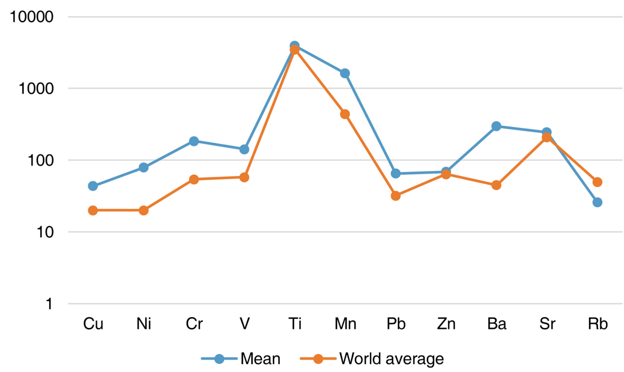

Fig. 3 Average abundance of trace elements in the soils of the study area and its comparison with world average soil composition (values after Alloway 2005; Pendias and Pendias 2001)

MgO. It is important to note that CaO* represents CaO, associated with silicate rocks. The molecular amount of CaO is recalculated after substituting the correspondent moles of CaO, consumed in calcite and apatite, furthermore, moles of Na_2O should be more than that of CaO. Depending upon the parent rock chemistry and type of weathering and alteration process, several weathering indices have been developed in the past. Some significant and most commonly used indices are CIA, CIW, PIA, PWI, WIP, CIX, ICV, and RR (Tunçay et al. 2019).

4.3.1 Chemical index of alteration (CIA)

The assessed CIA values of the studied sample are shown in (Table 4). The CIA values vary from 72.65 to 84.29, with an average of 77.38. The majority of the samples have CIA values varying from 70 to 80, indicating a large amount of leaching of Na, K, and Ca, in contrast to the stable phase of Al and Ti. This represents the prevalence of a moderate degree of weathering in the study area, in the warm and humid climatic conditions.

The spatial distribution diagram nicely demonstrates the regime of the CIA in the Porali Plain (Fig. 4a). The soil samples, from west of Piaro Ridge have relatively low CIA values, possibly due to a high influx of carbonate material lowering the CIA. On the contrary, samples collected, close to Bela Ophiolite (BO), have high CIA, because mafic and ultramafic rocks of BO are susceptible to chemical weathering. In general, samples collected from the southern part of the study area also have high CIA values, possibly because of the tail of the Porali River, before it plunges into the Miani Hor.

4.3.2 Chemical index of weathering (CIW)

Considering the contradicting weathering behavior of potash feldspars, in contrast to plagioclases, Harnoisand Moore (1988), suggested the Chemical Index of Weathering (CIW), amending CIA by eliminating the content of K_2O from assessments. The calculated values of CIW vary from 77.67 to 90.37 with a mean of 84.43, the corresponding CIW values of the studied soil samples are slightly higher than the CIA, indicating nearly analogous weathering behavior for the different parent rocks. The high CIW value refers to increased weathering (Baldermann et al. 2021). The spatial distribution diagram of CIW is similar to CIA, except for the values, which are relatively high due to the elimination of K_2O in the calculation (Fig. 4b).

4.3.3 Plagioclase index of alteration (PIA)

The rocks of Bela Ophiolite in the study area are tholeiitic and deficient in K_2O (Bhat et al. 2021), therefore PIA is a more appropriate index in this study as it eliminates the role of K-bearing feldspar (orthoclase and microcline). Using the molar concentration of various oxides of the soils of the Polori Plain, the PIA varies from 76.01 to 89.62, with mean and median values of 82.89 and 83.41 respectively (Table 4). PIA readings often tend to be higher; however, PIA values close to the CIA values suggest minor contributions of K_2O during burial and diagenesis (Mangold et al. 2019). The distribution pattern of PIA is also quite comparable with both CIA and CIW (Fig. 4c).

4.3.4 Product of weathering index (PWI)

The calculated PWI values of the present study fluctuate from 81.19 to 88.67, with a mean of 84.31 (Table 4). The mean and median (84.17) are close, indicating the consistent type of weathering parameters. On this scale, PWI values < 50 will represent the optimum fresh value (Fiantis et al. 2010) because the nature of all the oxides is immobile. The spatial distribution pattern displays variation in PWI values (Fig. 4d), the shape of contours is different from CIA, CIW, and PIA because SiO_2, TiO_2, and Fe_2O_3 are considered. A high zone is located, near Kanar, where the Porali River enters the Porali Plain, where all weathered soils are dispersed into the foothill of the Haro Range, southwards. An elongated NS low PWI zone exists, parallel to Piaro Ridge, indicating that the sedimentary rocks of Mor Range are resistant to weathering, resulting in low PWI values.

4.3.5 Weathering index of parker (WIP)

Parker (1970) evaluated the feldspar dissolution process as a proxy for silicate weathering, considering hydrolysis reactions of albite, orthoclase, and anorthite, in comparison to olivine and pyroxenes. For this reason, WIP is applied

Table 4 Various geochemical indices of weathering, and elemental ratios of soils of the study area

S.#	CIA	CIW	PIA	PWI	WIP	CIX	ICV	RR	K_2O/AI_2O_3	Rb/K	Rb/Ti	Rb/Sr
GC	77.59	87.20	85.39	83.91	31.46	78.73	1.29	7.22	0.14197	0.0020	0.0083	0.1392
RD	81.58	86.88	85.97	81.19	25.58	84.44	1.71	6.97	0.07477	0.0012	0.0016	0.0503
JD	77.34	87.34	85.46	82.31	25.48	80.50	1.04	6.20	0.14802	0.0023	0.0124	0.1026
WN	72.65	77.67	76.01	81.71	39.19	80.75	2.20	6.76	0.08890	0.0017	0.0030	0.0726
GN	74.70	81.05	79.29	83.18	34.31	81.12	1.52	6.71	0.10501	0.0018	0.0059	0.1283
MK	74.29	79.82	78.20	83.01	29.40	81.76	1.13	6.31	0.09329	0.0019	0.0067	0.0740
TD	77.88	86.60	84.91	85.17	32.56	79.56	1.59	8.10	0.12920	0.0027	0.0087	0.1398
KD	75.06	83.10	81.07	83.16	37.62	76.81	1.51	6.53	0.12897	0.0020	0.0070	0.1322
QG	78.34	86.76	85.17	83.73	28.48	80.58	1.04	6.50	0.12389	0.0020	0.0082	0.1543
CH	78.63	85.78	84.35	87.58	30.14	78.83	1.74	9.81	0.10595	0.0030	0.0074	0.1220
SA	78.36	84.71	83.36	84.42	29.71	79.58	1.47	7.56	0.09572	0.0030	0.0083	0.1260
JK	74.93	81.07	79.38	82.50	31.18	80.18	1.17	6.23	0.10098	0.0022	0.0076	0.1366
JJ	75.94	82.07	80.49	88.67	26.17	76.65	1.17	10.33	0.09840	0.0020	0.0059	0.0769
AG	75.49	82.83	80.98	85.71	31.01	78.83	1.30	7.91	0.11730	0.0020	0.0064	0.1354
SR	78.01	84.93	83.47	84.22	30.41	80.68	1.59	7.58	0.10439	0.0019	0.0046	0.0827
ML	76.06	85.80	83.72	85.51	30.95	76.79	1.68	8.43	0.14933	0.0018	0.0053	0.1163
CA	73.46	80.95	78.79	86.32	32.34	74.93	1.62	9.18	0.12602	0.0023	0.0064	0.1223
KN	79.00	86.91	85.45	84.12	26.70	81.40	1.00	6.68	0.11518	0.0021	0.0093	0.0979
JS	79.55	84.85	83.77	82.88	33.00	81.09	1.50	6.64	0.07851	0.0016	0.0035	0.0702
TH	76.87	82.53	81.14	84.56	31.42	77.38	1.30	7.25	0.08931	0.0028	0.0075	0.1143
DK	77.88	88.15	86.35	83.12	31.03	78.99	1.34	6.74	0.14960	0.0020	0.0077	0.1514
HA	78.34	83.50	82.34	87.87	18.25	84.65	0.94	8.93	0.07887	0.0021	0.0091	0.0497
PB	80.37	85.76	84.74	85.44	22.57	83.82	1.05	7.70	0.07819	0.0022	0.0067	0.0873
MH	84.29	90.37	89.62	82.58	24.34	84.63	0.99	5.81	0.07985	0.0019	0.0075	0.0592
LD	77.78	84.14	82.73	84.92	28.96	79.57	1.18	7.43	0.09722	0.0029	0.0085	0.1587
Mean	77.38	84.43	82.89	84.31	29.69	80.09	1.36	7.42	0.10795	0.1080	0.0069	0.1080
Minimum	72.65	77.67	76.01	81.19	18.25	74.93	0.94	5.81	0.07477	0.0748	0.0016	0.0748
Maximum	84.29	90.37	89.62	88.67	39.19	84.65	2.20	10.33	0.14960	0.1496	0.0124	0.1496
Median	77.69	84.78	83.41	84.17	30.28	80.13	1.32	7.22	0.10470	0.0020	0.0100	0.1153

on acid to basic igneous rocks and is more appropriate in this study with exposed diverse types of rock in the study area. WIP value ranges from 0 to 100 (Nadłonek and Bojakowska 2018); with values less than 50 indicating intense weathering, while values exceeding 50, represent the least weathered soil (Perri 2020). This interpretation of WIP value is contrary to CIA, PIA, and CIW values. The average WIP value of the studied samples is 29.69 (with a minimum value of 18.25 and a maximum value of 39.19). The median PIA value of 30.28 (Table 4) indicates moderate weathering in the study area.

4.3.6 *Modified chemical index of alteration (CIX)*

In the study area, carbonate rocks are exposed along with igneous rock (Fig. 1). This may affect the assessment of the degree of weathering because high CaO from carbonate rocks lowers the CIA value giving the wrong impression of the prevalence of weathering conditions in the area. The basic statistical analysis showed that the CIX of the soils of the study area ranged from 74.93 to 84.65, with a mean of 80.09 (Table 4), indicating moderate to high weathering. Two low zones of CIX exist to the west of Bela Town, close to Haro Range, and in front of Uthal Town (Fig. 4e).

4.3.7 *Index of compositional variability (ICV)*

The ICV values for the studied samples range from 0.94 to 2.20, reflecting variability in sediment maturity. Xu et al. (2020) indicated that sediments having ICV values > 1 are immature, while ICV value < 1 shows compositionally mature sediments. The mean ICV value of the studied samples is 1.36, indicating the existence of parent rock-forming minerals in the soil. The iso-concentration diagram

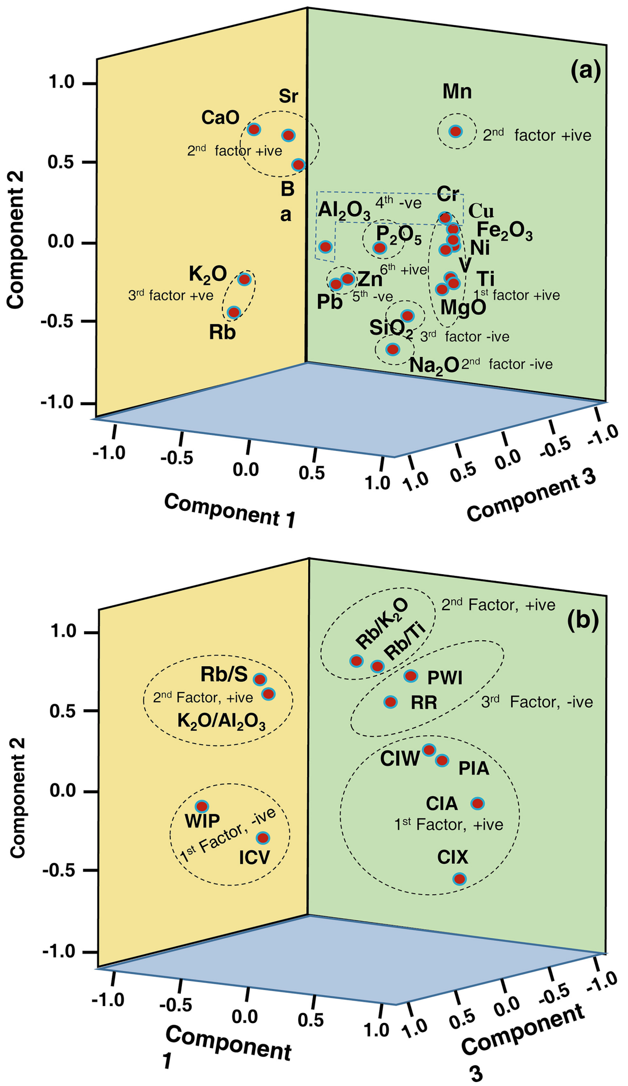

Fig. 4 Component plots of principal component analysis (PCA) on rotated space diagram, **a** major and trace elements, **b** weathering indices and elemental ratios

of ICV (Fig. 4f) also demonstrates a few patches of low ICV, located in the southern part of the Haro Range, north of Bela Town and at Uthal, reflecting relatively high weathering.

4.3.8 Ruxton ratio (RR)

Ruxton (1968) proposed a simple weathering index, which has been termed the Ruxton Ratio. The relative mobilities and loss of elements during weathering are evaluated by the simple mole ratio of SiO_2/AI_2O_3. The molar ratio of soils of the Porali Plain shows a deviation from 5.81 to 10.33, with a mean value of 7.42, reflecting variation in the weathering intensity. The ratio > 10 is indicative of optimum fresh value, while close to zero is the reflection of weathering (Price and Velbel 2003).

4.3.9 K_2O/AI_2O_3 ratio

Hou et al. (2021) used K_2O/AI_2O_3 ratio to portray the type of clay mineral, formed due to chemical weathering. A high ratio indicates the presence of illite while kaolinite-bearing soil has a low ratio. The K_2O/AI_2O_3 ratio of the soils of the Porali Plain ranges from 0.07477 to 0.14960, with an average of 0.10795 (Table 4). Nearly 56% of samples bear a ratio > 0.1, signifying the presence of illite clay in the soils of the study area, while the rest (44%) are kaolinite-rich (< 0.1).

4.3.10 Rb-type indices

Although rubidium (Rb) and K are analogues in geochemical character, Rb is less mobile, thus Rb/K_2O ratio increases with the progression of the soil formation process (Négrela et al. 2018). Dinis et al. (2016) elaborate on the role of rubidium (Rb), in contrast to K and Ti, and suggests using Rb/K_2O and Rb/Ti ratios to delineate the extent of weathering. A high Rb/K_2O ratio is noteworthy to designate the intensity of weathering. The current study shows an increase in ratio from 0.0747 to 0.1496, in different soil samples. The iso-concentration map of the Rb/K_2O ratio shows a high patch close to the course of the Porali River (Fig. 4g). On the eastern side, a north–south trending low ratio zone is also present, parallel to Piaro Ridge, the siliciclastic and carbonate rocks of Mor Range are unable to substantially contribute K_2O and Rb in the soils, in contrast to ophiolitic rocks of Bela Ophiolite. The Rb/Ti ratio decreases with weathering and can also be utilized to pinpoint the level of weathering. The Rb/Ti ratio of the studied samples varies from 0.0016 to 0.0124, soils with a low ratio show a high intensity of weathering. The relatively small size of Sr (1.32 Å), as compared to Rb (1.66 Å), helps leach out clay minerals from the exchange sites (Perri 2020). The studied soil samples are characterized by a low Rb/Sr ratio (av. 0.1079) affirming the prevalence of moderate level of weathering processes in the study area (Table 4). The Rb/Sr ratio of the entire study area depicted three distinct zones, from high to low (Fig. 4h). The first low Rb/Sr ratio zone is located, in the south-eastern part of the study area, where rocks of Bela Ophioliteare exposed. This area shows a relatively high density of small streams, responsible for the weathering of rocks, probably inducing more Sr during weathering (Kaleem et al. 2021). The second small low zone is located in the central part of the study area, fed by streams contributing high Sr, leached from the sedimentary rocks. The third low Rb/Sr region is confined along the eastern foothills of the Haro Range, where high Sr is related to the weathering of Nal Limestone, which is reefal and contains algae and corals.

4.4 Multivariate analysis of evaluated parameters

The correlation matrix provides insight into the abundance and origin of trace elements (Table 5). It is important to calculate sampling adequacy first, before doing multivariate statistical analysis. The correlation of the first input variables is necessary for factor analysis. Kaiser–Meyer–Olkin (KMO), a measure of sampling adequacy criteria is employed to assess how dependent the input variables are on one another (Durana et al. 2019). KMO values range between 0 and 1. Values ≥ 0.8 represent adequate sampling, 0.7–0.79 are middling, 0.6–0.69 are mediocre, and < 0.6 indicates insufficient sampling with value < 0.5 potentially leading to a factor analysis that will surely not be very useful for the examination of the data. KMO values also depend on the sample size; if the sample quantity is < 100, KMO values > 0.6 are acceptable for further factor analysis (Shrestha 2021). In this study, KMO has a value of 0.605 (Table 6) which is applicable for factor analysis. Bartlett's sphericity test is used to determine the strength of correlations among the data set to decide the utilization of dimension-reduction methods like principle components or common factor analysis. The significant value < 0.05 of Bartlett's sphericity test indicates that factor analysis may be worthwhile for the data set (Durana et al. 2019). The value of Bartlett's sphericity test for the studied samples is less than 0.05 (Table 6) supporting the principal component analysis (PCA).

Variance percent and loading values of PCA are valuable to infer the composition of host rocks, trace element assemblage, and their genetic affiliation (Table 7 and Fig. 5a). Strong correlation among Fe_2O_3 and MgO ($r = 0.722$) shows, the presence of basaltic rocks, associated with Bela Ophiolite. This segment of ophiolite can host several ore deposits (Edgar et al. 2022). This assumption is supported by the very strong correlation between Fe_2O_3 and Ti ($r = 0.907$), V ($r = 0.896$), and Cu ($r = 0.892$), furthermore, MgO also displays a very strong to moderate relation with Ti ($r = 0.805$), V ($r = 0.752$), Cu ($r = 0.608$), and Ni ($r = 0.548$). Very Strong correlation among Ti-V ($r = 0.961$), Cu-V ($r = 0.806$), and strong to moderate relation of Cu with Ti ($r = 0.791$) and Mn ($r = 0.625$), indicates the presence of volcanogenic massive sulfide (Domínguez-Carretero et al. 2022). The first factor accounts for 32.66% variance, with strong loading of Fe_2O_3 (0.936), Ti (0.918), and MgO (0.798), signifying their relevancy with the mafic rocks of BelaOphiolite. The second factor of PCA has a variance of 15.25%, with good loading of CaO (0.659), Sr (0.565), and Ba (0.475) indicating genetic linkage with Sedex and MVT-type mineralization in the Mor Range. The variance of the third factor is low (13.73%) and only K_2O (0.825) and Rb (0.669) are significant to designate the intensity of weathering. The variance percent and loading value of major and trace elements, displayed on the PCA rotated space diagram more precisely reveal the genetic linkage between them (Fig. 5a).

Heidari et al. (2022) emphasize the use of a correlations matrix and delineating different weathering indices to get a better understanding of immobile/mobile groups. Very strong correlations (Table 8) exist among CIA and CIW ($r = 0.833$); CIA and PIA ($r = 0.888$); CIW and PIA ($r = 0.994$); and PWI and Ruxton Ratio ($r = 0.911$). A strong correlation is found among WIP and ICV ($r = 0.701$); CIA and CIX ($r = 0.609$); CIX and Rb/Sr ($r = 0.648$) and Rb/K_2O and Rb/Ti ($r = 0.607$). The positive significant correlation of different weathering indices shows a uniform environment of weathering in the study area with identical conduct of mobile/immobile oxide groups. In contrast, the correlation coefficients of some of the measured weathering indices are negative (Table 8). The relation of WIP and CIA is ($r = -0.613$), WIP and CIX ($r = -0.569$); CIX and K_2O/AI_2O_3 ($r = -0.595$); ICV and Rb/Ti ($r = -0.647$) and CIX and Rb/Sr ($r = -0.584$). The negative correlation can be explained based on contrary weathering values of WIP to CIA, PIA, and CIW indexes (Perri 2020).

Weathering indices are further evaluated, using Principal component analysis (PCA). High loading of the first factor (33.94%) signifies a good relation with CIA (0.918), PIA (0.835), and CIW (0.786) plotted close to each other in the rotated space diagram (Table 9and Fig. 5b). The second factor (25.14%) has moderate loading with K_2O/AI_2O_3 (0.610), Rb/ K_2O (0.732), Rb/Ti (0.783), and Rb/Sr (0.676) plotted close to each other (Table 9 and Fig. 5b). The weight of the third factor is low (18.13%), and the loading of PWI and Ruxton Ratio is negative (-0.780) and (-0.777) respectively and plotted in the center (Table 9 and Fig. 5b).

4.5 Elements accumulation and contamination evaluation

Soil pollution is a serious issue because of the capability of toxic elements in soil, to be relocated into the human food chain through various conduits (Rinklebe et al. 2019). According to Gao et al. (2021), soil quality is a vital factor in controlling variable agricultural revolution. This study not only focuses on revealing the geochemical anomaly in the study area which affects the soil quality but also focuses on the appraisal of toxic elements that are present to attain better environmental health management (Kazapoe and Arhin 2021). The term geochemical background (GB) is used to discriminate the natural quantity of a given constituent in the environment from the extent originated because of human activity (Gałuszka 2007). Although the

Table 5 Correlation matrix of major and trace elements of soils of Porali Plain, Balochistan

	Al_2O_3	Fe_2O_3	MgO	CaO	Na_2O	K_2O	P_2O_5	Cu	Ni	Cr	V	Ti	Mn	Pb	Zn	Ba	Sr	Rb
SiO_2	− 0.459•	− 0.151	0.007	− 0.829•••	0.384	− 0.346	− 0.059	− 0.21	0.196	− 0.011	− 0.043	− 0.028	− 0.152	0.131	− 0.1	− 0.286	− 0.234	− 0.029
Al_2O_3		0.128	0.108	0.148	0.126	0.174	0.311	0.155	− 0.162	0.196	0.066	− 0.002	− 0.167	− 0.017	0.043	− 0.054	− 0.111	− 0.014
Fe_2O_3			0.722**	− 0.339	0.084	− 0.038	0.374	0.892***	0.409*	0.37	0.896***	0.907***	0.533*	− 0.157	0.411*	0.013	− 0.397	− 0.179
MgO				− 0.478•	0.313	− 0.062	0.486*	0.608**	0.548*	0.332	0.752**	0.805***	0.215	− 0.112	0.389	− 0.121	− 0.31	− 0.126
CaO					− 0.54•	0.292	− 0.248	− 0.22	− 0.38	− 0.217	− 0.426•	− 0.441•	0.021	− 0.07	− 0.12	0.336	0.468*	0.088
Na_2O						− 0.08	− 0.138	0.047	0.317	0.127	0.193	0.248	− 0.326	0.056	0.037	− 0.312	− 0.408•	0.083
K_2O							− 0.082	− 0.036	− 0.343	− 0.349	0.078	0.043	− 0.407•	0.036	0.251	0.323	− 0.107	0.738**
K_2O								0.366	0.073	− 0.005	0.365	0.358	0.113	0.091	0.138	0.038	− 0.029	− 0.031
Cu									0.346	0.269	0.806***	0.791***	0.625**	− 0.118	0.304	0.17	− 0.239	− 0.278
Ni										0.347	0.321	0.434*	0.318	− 0.238	0.079	0.123	− 0.158	− 0.325
Cr											0.306	0.304	0.33	0.026	− 0.138	− 0.299	− 0.39	− 0.543•
V												0.961***	0.41*	− 0.047	0.299	− 0.122	− 0.549•	− 0.139
Ti													0.359	− 0.101	0.304	− 0.043	− 0.515•	− 0.139
Mn														− 0.219	0.07	0.121	0.006	− 0.637••
Pb															0.253	− 0.146	− 0.252	− 0.002
Zn																0.096	− 0.211	0.302
Ba																	0.501*	0.156
Sr																		0.040

Value 0.8–1—***VeryStrong Positive Correlation—•••VeryStrong Negative Correlation

Value 0.6–0.79—**Strong Positive Correlation—••Strong Negative Correlation

Value 0.4–0.59—*Moderate Positive Correlation—•ModerateNegative Correlation geochemical background of trace elements still requires a thorough investigation, the values of upper continental crust element concentration are used by many authors in the calculation of quantitative indices for soil quality evaluation as geo-accumulation index (Rudnick and Gao 2003; Gałuszka et al. 2016; Bam et al. 2020; Parvez et al. 2023; Santos et al. 2023). The elemental abundances of the upper continental crust established by Kabata-Pendias (2011) were used as background values in this study (Table 3).

4.5.1 *Geo-accumulation index (I_{geo})*

The I_{geo} is an appropriate method for the evaluation of soil contamination only for a single heavy metal contaminant. Zhao et al. (2021) suggested seven pollution classifications of I_{geo} listed in Table 10. According to the classification presented in Table 10, most of the samples lie in class 0, followed by class 1. There are few exceptions, especially in the case of Pb and Ni which are marked as the greatest to moderately contaminated elements among the studied samples. This is probably due to the reported mineralization of these elements in the area (Shahab et al. 2016). During the obduction of BelaOphiolite, the Jurassic rock of the study area underwent intense tectonism and the incorporation of hydrothermal fluid responsible for the deposition of both sulfide-hosted (SEDEX/MVT) Pb–Zn mineralization within the sedimentary rocks of the study region.

4.5.2 *Improved nemerow index (IN)*

The $I_N$divulges the widespread pollution of each pollutant to the environment and provides a better picture for interpretation (Guan et al. 2014). To be consistent with I_{geo}, the classification of I_N was adjusted based on the results proposed by Förstner et al. (1990). The $I_N$values validate lead (Pb) being reported as a prime toxic element in the soils of the study area followed by Ti, Cr, and Ni (Table 11).

Table 6 KMO and Bartlett's Test values for present study

KMO and Bartlett's Test		
Kaiser–Meyer–Olkin Measure of Sampling Adequacy		0.605
Bartlett's Test of Sphericity	Approx. Chi-Square	158.552
	df	55
	Sig	.000

Table 7 Loadings of significant principal components for the major and trace elements of soils of the study area

	Component					
	1	2	3	4	5	6
SiO_2	0.021	− 0.585	− 0.579	0.438	− 0.121	0.159
Al_2O_3	0.044	− 0.022	0.344	−0.739	0.338	0.194
Fe_2O_3	0.936	0.056	0.245	− 0.007	0.000	−0.046
MgO	0.798	− .235	.156	.016	0.241	0.183
CaO	− 0.487	0.659	0.357	− 0.244	− 0.015	− 0.223
Na_2O	0.204	− 0.712	− 0.160	− 0.014	0.321	− 0.198
K_2O	− 0.220	− 0.170	0.825	0.039	− 0.020	− 0.295
P_2O_5	0.384	− 0.013	0.240	− 0.140	.064	0.822
Cu	0.866	0.227	0.237	0.007	− 0.006	0.008
Ni	0.556	− 0.030	− 0.298	0.299	0.409	− 0.062
Cr	0.477	0.024	− 0.407	− 0.510	0.072	− 0.211
V	0.905	− 0.137	0.239	− 0.033	− 0.064	− 0.087
Ti	0.918	− 0.157	0.227	0.062	0.035	− 0.092
Mn	0.605	0.667	− 0.260	0.070	− 0.196	− 0.054
Pb	− 0.093	− 0.315	0.029	− 0.210	− 0.714	0.214
Zn	0.318	− 0.168	0.495	0.180	− 0.376	0.054
Ba	− 0.073	0.475	0.420	0.475	0.177	0.057
Sr	− 0.463	0.565	0.033	0.322	0.264	0.318
Rb	− 0.397	− 0.417	0.669	0.274	0.050	− 0.065
% of Variance	32.66	15.25	13.73	8.06	6.27	5.65
Cumulative %	32.66	47.91	61.64	69.70	75.97	81.62

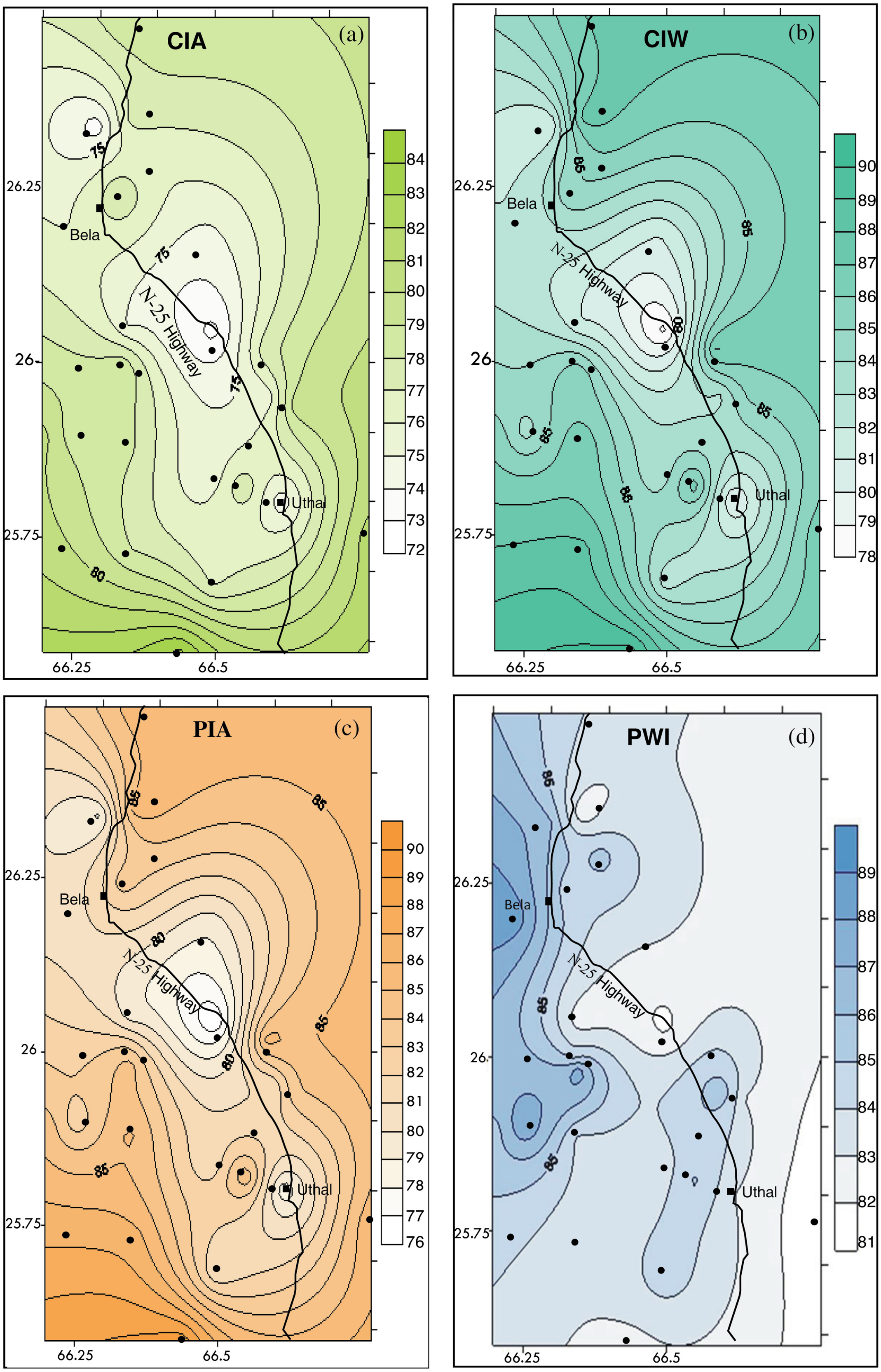

Fig. 5 Spatial distribution maps of weathering indices **a** CIA, **b**, CIW, **c** PIA, **d**, PWI, **e** CIX, **f** ICV, **g** Rb/K_2O and **h** Rb/Sr

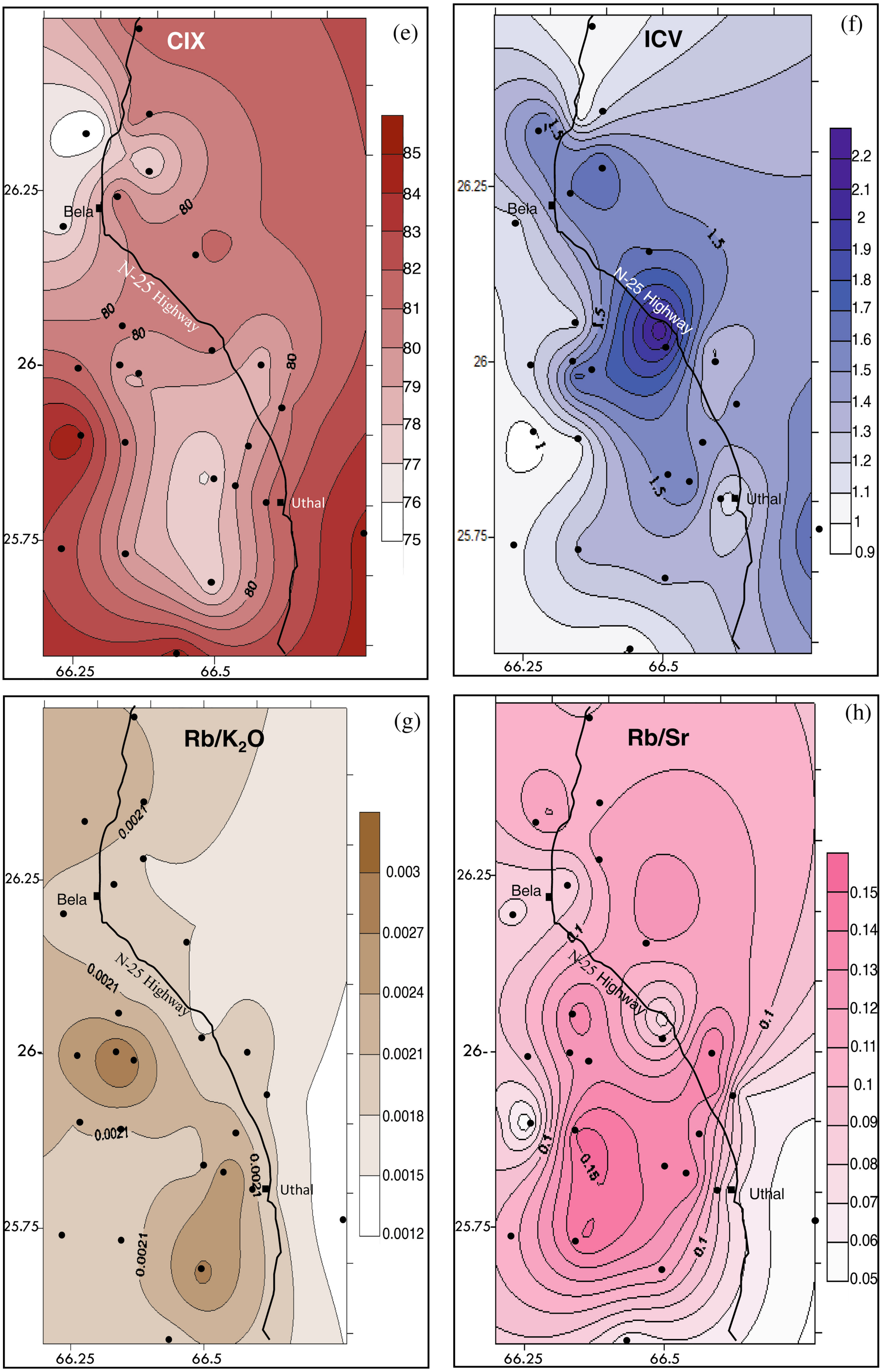

Fig. 5 continued

Table 8 Correlation matrix of geochemical indices and elemental ratios of the studied soils

	CIW	PIA	PWI	WIP	CIX	ICV	RR	K_2O/AI_2O_3	Rb/K_2O	Rb/Ti	Rb/Sr
CIA	0.833***	0.888***	− 0.085	− 0.613••	0.609**	− 0.361	− 0.153	− 0.324	− 0.026	0.070	− 0.313
CIW		0.994***	− 0.080	− 0.450•	0.282	− 0.344	− 0.154	0.253	0.034	0.327	0.058
PIA			− 0.087	− 0.494•	0.359	− 0.357	− 0.162	0.146	0.023	0.288	− 0.015
PWI				− 0.332	− 0.343	− 0.153	0.911***	0.019	0.445*	0.206	0.061
WIP					− 0.569••	0.701**	− 0.184	0.306	− 0.029	− 0.339	0.428*
CIX						− 0.312	− 0.408•	− 0.595••	− 0.336	− 0.070	− 0.584
ICV							0.186	0.045	− 0.126	− 0.647••	0.002
RR								0.012	0.321	− 0.065	− 0.025
K_2O/AI_2O_3									0.098	0.428*	0.648**
Rb/K_2O										.607**	0.499*
Rb/Sr											0.412*

Value 0.8–1—***VeryStrong Positive Correlation—•••VeryStrong Negative Correlation

Value 0.6–0.79—**Strong Positive Correlation—••Strong Negative Correlation

Value 0.4–0.59—*Moderate Positive Correlation—•ModerateNegative Correlation

Table 9 Loadings of significant principal components of weathering indices for the soils of the study area

	Component			
	1	2	3	4
CIA	0.918	− 0.022	− 0.009	0.298
CIW	0.786	0.333	0.307	0.419
PIA	0.835	0.271	0.256	0.402
PWI	− 0.120	0.551	− 0.780	0.163
WIP	− 0.787	− 0.149	0.484	0.164
CIX	0.735	− 0.507	− 0.072	− 0.236
ICV	− 0.615	− 0.364	0.089	0.567
RR	− 0.267	0.372	− 0.777	0.407
K_2O/AI_2O_3	− 0.266	0.610	0.536	0.207
Rb/K_2O	− 0.100	0.732	− 0.182	− 0.164
Rb/Ti	0.274	0.783	0.135	− 0.466
Rb/Sr	− 0.368	0.676	0.467	− 0.019
% of Variance	33.94	25.14	18.13	10.91
Cumulative %	33.94	59.08	77.21	88.12

4.6 Repercussion in agriculture

4.6.1 Lead (Pb)

The average amount of Pb in the soil is 32 mg/kg (Alloway 2005) however, in the soil of the study area, the range of Pb was observed as 14–342 with a mean value of 65.3 mg/kg (Table 3). The soil–plant relation can be used to identify the transfer factor (TF) of a toxic element. The TF can be assessed by calculating the ratio of the element in the plant and the soil (Tasrina et al. 2015). Tepanosyan et al. (2022) assessed the TF of 12 common fruits and vegetables in the Republic of Armenia and found a high level of bioaccumulation of Pb in their studied samples. Both the studied contamination indices; I_{geo} (28%) and I_N (2.20) point out Pb as a moderately to heavily contaminated element (Tables 10 and 11). The higher content of Pb (> 400 mg/kg) in agricultural soil is a risk to human health (Yang et al. 2019). Common crops can tolerate up to 100 mg/kg (Misenheimer et al. 2018). High exposure to Pb, causes noxious effects on crop production and reduces germination of seeds, due to intervention with enzymes and damage of membrane (Collin et al. 2022). Lead is the second most toxic metal having a role in the biological activity of plants after arsenic (Table 1). It reduces seed germination, induces structural changes in photosynthetic apparatus, and reduces biosynthesis of chlorophyll pigments causing retardation of carbon metabolism (Zulfiqar et al. 2019). Soybean, wheat, spinach, cabbage, and peas are more sensitive to high Pb in the soil (Osman and Fadhlallah2023). High amounts of Pb are likely due to the sulphide mineralization of Pb–Zn in the adjacent Mor Range (Arain et al. 2021; Shahab et al. 2016).

4.6.2 Nickel (Ni)

Nickel is among trace elements that are considered toxic for living organisms if present in agricultural soils (Kayode et al. 2022). Normally the amount of Ni is found in trace quantities (20 to 30 mg/kg) but in the study area, it ranges from 43 to 143 mg/kg with an average of 79 mg/kg (Table 3). The assessed geo-accumulation index signifies

Table 10 Classification of Geo-Accumulation Index by Müller (1969)

I_{geo}	Class	Sediment quality	Cu	Ni	Cr	V	Ti	Pb	Zn	Ba	Sr	Rb
< 0	0	Absence of contamination	92%	4%	Nil	92%	100%	52%	92%	96%	64%	100%
0–1	1	From absent to moderately contaminated	8%	64%	68%	8%		20%	8%	4%	36%	
1–2	2	Moderately contaminated		32%	32%			12%				
2–3	3	From moderate to heavily contaminated						12%				
3–4	4	Heavily contaminated						4%				
4–5	5	From heavily to extremely contaminated										
> 5	6	Extremely contaminated										

Table 11 Classification of Nemerow pollution Index (**I_N**) proposed by Förstner et al. (1990)

Class	I_N Values	Sediment quality	Present Study
0	$0 < I_N \leq 0.5$	Uncontaminated	Sr (0.48), Zn (0.42) V (0.37)
1	$0.5 < I_N \leq 1$	Uncontaminated to moderately contaminated	Ba (0.92), Cu (0.54)
2	$1 < I_N \leq 2$	Moderately contaminated	Ti (1.8), Ni (1.26), Cr (1.23), Rb (1.03)
3	$2 < I_N \leq 3$	Moderately to heavily contaminated	Pb (2.20)
4	$3 < I_N \leq 4$	Heavily contaminated	–
5	$4 < I_N \leq 5$	Heavily to extremely contaminated	–
6	$I_N > 5$	Extremely contaminated	–

the second contaminated element according to (I_{geo}) and (I_N) values (Tables 10 and 11). The Ni is integrated from ultramafic rocks (Korobkin et al. 2022). The elevated amount of Ni in the studied samples is due to the weathering of ultramafic rocks present in the surrounding region. The concentration of Ni in plants is very low, ~ 1.5 µg/gm, which is considered a safe limit in the crops. The higher level may shunt the entire parts of the plant, including, roots, shoots, leaves, etc. by poisoning enzymes (Khan et al. 2023; Mustafa et al. 2023). This is reflected by means of chlorosis, necrosis, and a decline in water content (Naz et al. 2022).

4.6.3 Chromium (Cr)

Chromium uptake and translocation are largely based on the chemical speciation of Cr, which mainly exists as either Cr^{3+} or Cr^{6+}, depending upon the redox potential, organic matter, and soil pH. Both Cr^{3+} & Cr^{6+} are highly stable and precipitate at pH > 5.5 (Wu et al. 2022). Among them, Cr^{6+} occurs as oxyanions and has more impact on toxicity in crops (Wani et al. 2022). Chromium is known to be a toxic metal that can pollute agricultural soil and cause damage to plants (Zhang et al. 2020a). It is most abundant in ultramafic rocks and can be transported by surface runoff in its soluble or precipitated form (Havryliuk et al. 2022). In the studied soil samples, Cr ranges from 129 to 286 mg/kg, while the mean value is 184 mg/kg (Table 3), which is much higher than the world average of 54 mg/kg (Alloway 2005). In the studied soil samples, the I_{geo} value of Cr was reported in 32% of soil samples as moderately contaminated; the I_N value (1.23) also confirms Cr is the third pollutant in the studied samples (Tables 10 and 11). The Cr provokes harmful influences on some physiological and morphological functions of crops (Table 1). A high quantity of Cr can reduce plant growth, induce chlorosis, reduce pigment content, and alter enzymatic functions, damage root cells, chloroplast, and cell membrane (Saleem et al. 2022; Ao et al. 2022). The toxic effects of Cr are correlated with the generation of reactive oxygen species (ROS), which cause oxidative stress in plants (Sharma et al. 2020).

4.6.4 Strontium (Sr)

The studied samples showed a considerable amount of Sr (187–351) with a mean value of 237 mg/kg, which is higher than the world's average abundance (120 mg/kg) in the soil (Sposito 2008). The general concentration of Sr varies from 15 to 1,000 mg/kg, largely depending on the physicochemical and mineralogical characteristics of the soil, soil acidity, and organic content (Dubchak 2018). The studied samples showed a considerable amount of Sr, and the I_{geo} value of 36% of the soil sample shows moderate contamination. However, according to I_N all samples are uncontaminated (Tables 10 and 11). High Sr in the soil can replace Ca due to its chemical similarity and cause a lack of Ca in the plants (Burger and Lichtscheidl 2019). In soil, the heavier strontium occurs as a less mobile hydroxide, which results in its accumulation in soil and plant tissues (Abdel-Sabour 2022). The biological function of alone stable $^{87}Sr^{2+}$ in the crops is not mentioned in the available literature; however, its biogeochemical behavior is analogous to Ca^{2+} because both Ca^{2+} and Sr^{2+} belong to the 2nd group of the periodic table (Zhang et al. 2020b). High Sr^{2+} in the soil can replace Ca^{2+} and cause a lack of Ca in the plants (Burger and Lichtscheidl 2019). The high content of Sr^{2+}in the plants is associated with a decrease in chlorophyll content (Srikhumsuk et al. 2023).

5 Conclusions

The present study confirms the presence of loamy soils in the Porali Plain. Inferences show that major and trace elements accumulated in studied soils are due to rock weathering and alteration in Bela Ophiolite and Ferozabad Group. Enrichment of a few toxic elements was also in the retort of VMS, Sedex, and MVT types of mineralization in the studied region. Weathering indices determined a moderate to high degree of weathering with the existence of illite clay in association with kaolinite in the soils of the study area. Spatial distribution patterns of different indices and ratios demarcate the zones of high to low weathering and indicate suitable areas for agriculture. Geo-accumulation and Improved Nemerow indices revealed Pb as a prime toxic element followed by Ti, Ni, and Cr.

Acknowledgements This work was supported by the Dean Faculty of Science, University of Karachi research grant. We extend our appreciation to Mr. Shabbir Ahmed Baloch, proprietor of Industrial Mineral Grinding, Marble City, Hub, Balochistan for his cooperation during the fieldwork. The authors are highly indebted to the hospitability of the inhabitants and farmers of the area for their cooperation and for collecting soil samples.

Author contributions MK acts as a team leader to organize the present work, collection of soil samples and their analysis, interpretation and drafting manuscript. EB managed the analytical data, created spatial patterns, and supported in interpretation. SN analyzed soil samples and helped to assess the weathering Indices. TR assessed XRF analysis and BS contributed to the geology of the study area.

Data availability The authors declare that all relevant data are included in the article and/or in its supplementary information files.

Declarations

Conflict of interest The authors declare no competing interests.

Ethical approval Not applicable.

References

AbdElgawad H, Mohammed AE, van Dijk JR, Beemster GTS, Alotaibi MO, Saleh AM (2023) The impact of chromium toxicity on the yield and quality of rice grains produced under ambient and elevated levels of CO_2. Front Plant Sci 14:1019859. https://doi.org/10.3389/fpls.2023.1019859

Abdel-Sabour MF (2022) Fate of cesium and strontium in soil-to-plant system (Overview). J Rad Nucl Appl 7(2):78–93. https://doi.org/10.18576/jrna/07021

Ahmadi A, Emami M, Daccache A, He L (2021) Soil properties prediction for precision agriculture using visible and near-infrared spectroscopy: a systematic review and meta-analysis. Agronomy 11(3):433. https://doi.org/10.3390/agronomy11030433

Ali S, Mir RA, Tyagi A, Manzar N, Kashyap AS, Mushtaq M, Raina A, Park S, Sharma S, Mir ZA (2023) Chromium toxicity in plants: signaling, mitigation, and future perspectives. Plants 12:1502. https://doi.org/10.3390/plants1207150

Alloway BJ (2005) Bioavailability of Elements in soil. In: Selinus O (ed), Essential of medical geology, impacts of the naturak environment on public health pp 347–372, Elsevier Academic Press Amsterdam

Ao M, Chen X, Deng T, Sun S, Tang Y, Morel JL, Qiu R, Wang S (2022) Chromium biogeochemical behavior in soil-plant systems and remediation strategies: a critical review. J Hazard Mat 424:127233. https://doi.org/10.1016/j.jhazmat.2021.127233

Arain AW, Mastoi AS, Hakro AAAD, Rajper RA, Jamali MA, Bhatti Bhatti GR, W (2021) A preliminary review on the metallogeny of sediment-hosted Pb-Zn deposits in Balochistan Pakistan. Earth Sci Malaysia 5(1):19–26. https://doi.org/10.26480/esmy.01.2021.19.26

Baldermann A, Dietzel M, Reinprecht V (2021) Chemical weathering and progressing alteration as possible controlling factors for creeping landslides. Sci Total Environ 778:146300. https://doi.org/10.1016/j.scitotenv.2021.146300

Bam EK, Akumah AM, Bansah S (2020) Geochemical and chemometric analysis of soils from a data scarce river catchment in West Africa. Environ Res Commun 2(3):035001

Bankaji I, Kouki R, Dridi N, Ferreira R, Hidouri S, Duarte B, Sleimi N, Caçador I (2023) Comparison of digestion methods using atomic absorption spectrometry for the determination of metal levels in plants. Separations. https://doi.org/10.3390/separations10010040

Barman U, Choudhury RD (2019) Soil texture classification using multi class support vector machine. Inform Pro Agri 7(2):318–332. https://doi.org/10.1016/j.inpa.2019.08.001

Bhat IM, Ahmad T, Rao DVS, Rao NVC (2021) Petrological and geochemical characterization of the arc-related Suru-Thasgamophiolitic slice along the Indus Suture Zone, Ladakh Himalaya. Geol Mag 158(8):1441–1460. https://doi.org/10.1017/S0016756821000042

Bhuiyan MAH, Karmaker SC, Bodrud-Doza M, Rakib MA, Saha BB (2021) Enrichment, sources and ecological risk mapping of heavy metals in agricultural soils of Dhaka district employing SOM, PMF and GIS methods. Chemosphere 263:128339. https://doi.org/10.1016/j.chemosphere.2020.128339

Burger A, Lichtscheidl I (2019) Strontium in the environment: Review about reactions of plants towards stable and radioactive strontium isotopes. Sci Total Environ 653:1458–11512. https://doi.org/10.1016/j.scitotenv.2018.10.312

Bykov VG, Merkulova TV (2022) Stress transfer and the impact of the India–Eurasia collision and the western pacific subduction on the geodynamics of the Asian continent. Open J Earthquake Res 11(4):73–88

Collin S, Baskar A, Geevarghese DM, Ali MNVS, Bahubali P, Choudhary R, Lvov V, Tovar GI, Senatov F, Koppala S, Swamiappan S (2022) Bioaccumulation of lead (Pb) and its effects in plants: a review. J Hazard Mater 3:100064. https://doi.org/10.1016/j.hazl.2022.100064

Cox R, Lowe DR, Cullers RL (1995) The influence of sediment recycling and basement composition on evolution of mudrock chemistry in the southwestern United States. Geochim Cosmochim Acta 59(14):2919–2940. https://doi.org/10.1016/j.hazl.2022.100064

da Silva RJAB, da Silva YJAB, van Straaten P, do Nascimento CWA, Biondi CM, da Silva YJAB, de AraújoFilho JC (2022) Influence of parent material on soil chemical characteristics in a semi-arid tropical region of Northeast Brazil. Environ Monit Assess 194(5):1–21. https://doi.org/10.1007/s10661-022-09914-9

DeclercqY DN, De Grave J, De Smedt P, Finke P, Mouazen AM, Nawar S, Vandenberghe D, Van Meirvenne M, Verdoodt A (2019) A comprehensive study of three different portable XRF scanners to assess the soil geochemistry of an extensive sample dataset. Remote Sens 11:2490. https://doi.org/10.3390/rs11212490

Deng K, Yang S, Guo Y (2022) A global temperature control of silicate weathering intensity. Nat Commun 13:1781. https://doi.org/10.1038/s41467-022-29415-0l

Dinis PA, Dinis JL, Mendes MM, Rey J, Pais J (2016) Geochemistry and mineralogy of the Lower Cretaceous of the Lusitanian Basin (western Portugal): deciphering palaeoclimates from weathering indices and integrated vegetational data. Comptes Rendus Geosci 348:139–149. https://doi.org/10.1016/j.crte.2015.09.003

Domínguez-Carretero D, Proenza JA, González-Jiménez JM, Llanes-Castro AI, Torres H, Aiglsperger T, Torró L, Capote C, Nuez D, Garcia-Casco A (2022) Ultramafic-hosted volcanogenic massive sulfide deposits from Cuban ophiolites. J South Amer Earth Sci 119:103991. https://doi.org/10.1016/j.jsames.2022.103991

Dubchak S (2018) Distribution of Strontium in Soil: Interception, weathering, ppeciation, and translocation to Plants. In: DK Gupta, C. Walther (eds.), Behaviour of Strontium in Plants and the Environment, 33–43. https://doi.org/10.1007/978-3-319-66574-0_3

Durana P, Kliestikova J, Kovacova M (2019) The quality of brand products: expected attributes vs. perceived reality. Econo Cult 16(1):98–107. https://doi.org/10.2478/jec-2019-0011

Edgar A, Sanislav IV, Dirks PHGM (2022) Tectonic setting and mineralisation potential of the Cowley Ophiolite Complex, north Queensland. Aust J Earth Sci. https://doi.org/10.1080/08120099.2022.2086173

El-Anwar A, Mekky HS, Abdel Wahab W, Asmoay AS, Elnazer AA, Salman SA (2019) Geochemical characteristics of agricultural soils, Assiut governorate. Egypt Bull Nat Res Centre 43(1):1–9. https://doi.org/10.1186/s42269-019-0080-3

Fedo CM, Nesbitt HW, Young GM (1995) Unraveling the Effects of potassium metasomatism in sedimentary rocks and paleosols, with implications for paleo weathering conditions and provenance. Geology 23:921–924. https://doi.org/10.1130/00917613(1995)023%3c0921:UTEOPM%3e2.3.CO;2

Fiantis D, Nelson M, Shamshuddin J, Ranst Goh TB, EV, (2010) Determination of the geochemical weathering indices and trace elements content of new volcanic ash deposits from Mt. Talang (West Sumatra) Indonesia. Eurasian Soil Sci 43(13):1477–1485. https://doi.org/10.1134/S1064229310130077

Förstner U, Ahlf W, Calmano W, Kersten, M (1990) Sediment criteria development. Sedi environ Geochem 311–338 pp Springer Berlin Heidelberg, DOI: https://doi.org/10.1007/978-3-642-75097-7_18

Gałuszka A (2007) A review of geochemical background concepts and an example using data from Poland. Environ Geol 52:861–870. https://doi.org/10.1007/s00254-006-0528-2

Gałuszka A, Migaszewski Z, Duczmal-Czernikiewicz A, Dołęgowska S (2016) Geochemical background of potentially toxic trace elements in reclaimed soils of the abandoned pyrite–uranium mine (south-central Poland). Int J Environ Sci Tech 13:2649–2662

Gao Z, Dong H, Wang S, Zhang Y, Zhang H, Jiang B, Liu Y (2021) Geochemical characteristics and ecological risk assessment of heavy metals in surface soil of Gaomi City. Int J Environ Res Pub Health 18(16):8329. https://doi.org/10.3390/ijerph18168329

Garzanti E, Padoan M, Setti M, López-Galindo A, Villa IM (2014) Provenance versus weathering control on the composition of tropical river mud southern Africa. ChemGeol 366:61–74

Gonçalves DAM, Pereira WVdS, Johannesson KH, Pérez DV, Guilherme LRG, Fernandes AR (2022) Geochemical background for potentially toxic elements in forested soils of the State of Pará. Brazil Amazon Minerals 12:674. https://doi.org/10.3390/min12060674

Guan Y, Shao C, Ju M (2014) Heavy metal contamination assessment and partition for industrial and mining gathering areas. Int J Environ Res Pub Health 11(7):7286–7303. https://doi.org/10.3390/ijerph110707286

Harnois LJM, Moore JM (1988) Geochemistry and origin of the ore chimney formation: a transported pale-oregolith in the Grenville province of Southeastern Ontario, Canada. ChemGeol 69:267–289. https://doi.org/10.1016/0009-2541(88)90039-3

Hasan O, Miko S, Mesić S, Peh Z (2023) Chemical weathering rates of soils developed on Eocene marls and sandstones in a Mediterranean catchment (Istria, Croatia). Land 12(4):913

Havryliuk O, Hovorukha V, Bida I, Danko Y, Gladka G, Zakutevsky O, Tashyrev O (2022) Bioremediation of copper-and chromium-contaminated soils using *Agrostiscapillaris L*, *Festucapratensis Huds*, and *Poapratensis L*. Mixture of Lawn Grasses Land 11(5):623. https://doi.org/10.3390/land11050623

Heidari A, Osatb M, Konyushkovac M (2022) Geochemical indices as efficient tools for assessing the soil weathering status in relation to soil taxonomic classes. CATENA 208:105716. https://doi.org/10.1016/j.catena.2021.105716

Hou H, Liu S, Shao L, Li Y, Wang ZM, C, (2021) Elemental geochemistry of the Middle Jurassic shales in the northern Qaidam Basin, northwestern China: constraints for tectonics and paleoclimate. Open Geosci 13:1448–1462. https://doi.org/10.1515/geo-2020-0318

HSC (1960) Hunting Survey Co. Ltd Reconnaissance Geology of Part of West Pakistan; a Colombo Plan-Co-Operative Project Canada

Hu B, Chen S, Hu J, Xia F, Xu J, Li Y, Shi Z (2017) Application of portable XRF and VNIR sensors for rapid assessment of soil heavy metal pollution. PloS One 12(2):0172438. https://doi.org/10.1371/journal.pone.0172438

Jalil R, Alard O, Schaefer B, Ali L, Sajid M, Khedr MZ, Shah MT, Anjum MN (2023) Geochemistry of waziristan ophiolite complex, Pakistan: implications for Petrogenesis and tectonic setting. Minerals 13:311. https://doi.org/10.3390/min13030311

Kabata-Pendias A, Pendias H (2001) Trace Elements in Soils and Plants, 3rd edn. CRC Press Inc, Boca Raton Florida, p 331

Kabata-Pendias A, Pendias H (2011) Trace Elements in Soils and Plants, 4th edn. CRC Press, Boca Raton

Kaleem M, Naseem S, Bashir E, Shahab B, Rafique T (2021) Discrete geochemical behavior of Sr and Ba in the groundwater of Southern Mor Range Balochistan, a Tracer for Igneous and sedimentary rocks weathering and related environmental issues. ApplGeochem 130:104996. https://doi.org/10.1016/j.apgeochem.2021.104996

Kayode OT, Ogunyemi EF, Odukoya AM, Aizebeokhai AP (2022) Assessment of chromium and nickel in agricultural soil: implications for sustainable agriculture. Earth Environ Sci 993(1):012–014. https://doi.org/10.1088/1755-1315/993/1/012014

Kazapoe R, Arhin E (2021) Determination of local background and baseline values of elements within the soils of the Birimian Terrain of the Wassa Area of Southwest Ghana. Geol Eco Landscapes 5(3):199–208. https://doi.org/10.1080/24749508.2019.1705644

Khan ZI, Ahmad K, Ahmad T, Zafar A, Alrefaei AF, Ashfaq A, Akhtar S, Mahpara S, MehmoodN UI (2023) Evaluation of nickel toxicity and potential health implications of agriculturally diversely irrigated wheat crop varieties. Arab J Chem 16(8):104934. https://doi.org/10.1016/j.arabjc.2023.104934

Korobkin V, Samatov I, Chaklikov A, Tulemissova Z (2022) Peculiarities of dynamics of Hypergenic mineral transformation of nickel weathering crusts of ultramafic rocks of the Kempirsay group of deposits in western Kazakhstan. Minerals 12(5):650. https://doi.org/10.3390/min12050650

Kumar S, Wang M, Liu Y, Fahad S, Qayyum A, Jadoon SA, Chen Y, Zhu G (2022) Nickel toxicity alters growth patterns and induces oxidative stress response in sweet potato. Front Plant Sci 13:1054924. https://doi.org/10.3389/fpls.2022.1054924

Laperche V, Lemière B (2021) Possible pitfalls in the analysis of minerals and loose materials by portable XRF, and how to overcome them. Minerals 11:33. https://doi.org/10.3390/min11010033

Liang Z, Zeng H, Kong J (2023) Contrasting responses and phytoremediation potential of two poplar species to combined strontium and diesel oil stress. Plants 12:2145. https://doi.org/10.3390/plants12112145

Mangold N, Dehouck E, Fedo C, Forni O, Achilles C (2019) Chemical alteration of fine-grained sedimentary rocks at Gale crater. Icarus 321:619–631. https://doi.org/10.1016/j.icarus.2018.11.004

Mao X, Sun J, Shaghaleh H, Jiang X, Yu H, Zhai S, Hamoud YA (2023) Environmental assessment of soils and crops based on heavy metal risk analysis in Southeastern China. Agronomy 13:1107. https://doi.org/10.3390/agronomy13041107

Martín MA, Pachepsky YA, García Gutiérrez C, Reyes C (2018) On soil textural classifications and soil-texture-based estimations. Solid Earth 9:159–165. https://doi.org/10.5194/se-2017-84

Misenheimer J, Nelson C, Huertas E, Medina-Vera M, Prevatte A, Bradham K (2018) Total and bioaccessible soil arsenic and lead levels and plant uptake in three urban community gardens in Puerto Rico. Geoscience 8(2):43. https://doi.org/10.3390/geosciences8020043

Müller G (1969) Index of geoaccumulation in sediments of the Rhine River. Geol J 2:108–118

Mustafa A, Zulfiqar U, Mumtaz MZ, Radziemska M, Haider FU, Holatko J, Hammershmiedt T, Naveed M, Ali H, Kintl A, Saeed Q, Kucerik J, Brtnicky M (2023) Nickel (Ni) phytotoxicity and detoxification mechanisms: a review. Chemosphere 328:138574. https://doi.org/10.1016/j.chemosphere

Nadłonek W, Bojakowska I (2018) Variability of chemical weathering indices in modern sediments of the Vistula and Odra Rivers (Poland). Appl Eco Environ Res 16(3):2453–2473. https://doi.org/10.15666/aeer/1603_24532473

Nadporozhskaya M, Kovsh N, Paolesse R, Lvova L (2022) Recent advances in chemical sensors for soil analysis: a review. Chemosensors 10:35. https://doi.org/10.3390/chemosensors10010035

Naz M, Ghani MI, Sarraf M, Liu M, Fan X (2022) Ecotoxicity of nickel and its possible remediation. Phytoremediation. https://doi.org/10.1016/B978-0-323-89874-4.00022-4

Négrela P, Ladenbergerb A, Reimannc C, Birked M, Sadeghib M (2018) Distribution of Rb, Ga and Cs in agricultural land soils at European continental scale (GEMAS): implications for weathering conditions and provenance. Chem Geol 479:188–203. https://doi.org/10.1016/j.chemgeo.2018.01.009

Nesbitt HW, Young GM (1982) Early proterozoic climates and plate motions inferred from major element chemistry of Lutites. Nature 299:715–717. https://doi.org/10.1038/299715a0

Osman HE, Fadhlallah RS (2023) Impact of lead on seed germination, seedling growth, chemical composition, and forage quality of different varieties of Sorghum. J Umm Al-QuraUnivAppllSci 9:77–86. https://doi.org/10.1007/s43994-022-00022-5

Pandarinath K (2022) Application potential of chemical weathering indices in the identification of hydrothermally altered surface volcanic rocks from geothermal fields. Geosci J 26(3):415–442. https://doi.org/10.1007/s12303-021-0042-2

Parikh SJ, James BR (2012) Soil: the foundation of agriculture. Nat Edu Know 3(10):2

Parker A (1970) An index of weathering for silicate rocks. Geol Mag 107:501–504. https://doi.org/10.1017/S0016756800058581

Parvez MS, Nawshin S, Sultana S, Hossain MS, Rashid K, Habib MA, Khan R (2023) Evaluation of Heavy Metal Contamination in Soil Samples around Rampal. ACS omega, Bangladesh

Perri F (2020) Chemical weathering of crystalline rocks in contrasting climatic conditions using geochemical proxies: an overview. Palaeogeog Palaeoclim Palaeoeco 556:109873. https://doi.org/10.1016/j.palaeo.2020.1098736

Price JR, Velbel MA (2003) Chemical weathering indices applied to weathering profiles developed on heterogeneous felsic metamorphic parent rocks. ChemGeol 202:397–416. https://doi.org/10.1016/j.chemgeo.2002.11.001

Rashid MU, Ahmed W, Waseem M, Zamin B, Ahmad M, Sabri MMS (2022) Metallic-mineral prospecting using integrated geophysical and geochemical techniques: a case study from the Belaophiolitic complex, Baluchistan. Pakistan Minerals 12(7):825

Rinklebe J, Antoniadis V, Shaheen SM, Rosche O, Altermann M (2019) Health risk assessment of potentially toxic elements in soils along the Central Elbe River, Germany. Environ Int 126:76–88. https://doi.org/10.1016/j.envint.2019.02.011

Rudnick RL, Gao S (2003) Composition of the continental crust. Treatise Geochem 3:1–64. https://doi.org/10.1016/b0-08-043751-6/03016-4

Ruxton BP (1968) Measures of the degree of chemical weathering of rocks. J Geol 76:518–527. https://doi.org/10.1086/627357

Sabouang JF, Ateba JFB, Shouop CJG, Maya J, Kamkumo CT, Mohamadou LL, Simo A (2023) Accuracy and precision of energy dispersive X-Ray fluorescence (EDXRF) analysis of trace and major elements in rock standard reference materials using fine powder. J of Geosci Environ Protect 11(6):83–95

Saleem MH, Afzal J, Rizwan M, Shah ZUH, Depar N, Usman K (2022) Chromium toxicity in plants: consequences on growth, chromosomal behavior andmineral nutrient status. Turkish J Agric For 46(3):371–389

Santos P, Ribeiro J, Espinha Marques J, Flores D (2023) Environmental and health risk assessment of soil adjacent to a self-burning waste pile from an abandoned coal mine in northern Portugal. Environ 10(3):53

Shahab B, Bashir E, Kaleem M, Naseem S (2016) Assessment of barite of Lasbela, Balochistan Pakistan, as drilling mud and environmental impact of associated Pb, As, Hg, Cd and Sr. Environ Earth Sci. https://doi.org/10.1007/s12665-016-5916-7

Shaltami OR, Bustany I (2021) Agricultural Geochemistry- A Review, 2nd International Symposium on Geosciences (ISG2021) 28–34 p. https://www.researchgate.net/publication/351126566, Shamkhi MS, Al-Badry HJ (2022) Soil texture distribution for East Wasit Province. Iraq Ear Environ Sci 961(1):012073

Sharma A, Kapoor D, Wang J, Shahzad B, Kumar V, Bali AS, Shivam J, Zheng B, Yuan H, Yan D (2020) Chromium bioaccumulation and its impacts on plants: an overview. Plants 9(1):100. https://doi.org/10.3390/plants9010100

Shrestha N (2021) Factor analysis as a tool for survey analysis. Am J Appl Math Stats 9(1):4–11. https://doi.org/10.12691/ajams-9-1-2

Siddiqui NK, Jadoon IAK (2013) Indo-Eurasian Plate collision and the evolution of Pak-Iran MakranMicroplate, Pishin-Katawaz Fault Block and the Porali Trough. PAPG/SPE ATC Islamabad, Pakistan AAPG, Search and Discovery Article #30265

Sirbu-Radasanu DS, Huzum R, Dumitras DG, Stan CO (2022) Mineralogical and Geochemical Implications of Weathering Processes Responsible for Soil Generation in Mănăila Alpine Area (Tulghe¸s 3 Unit—Eastern Carpathians). Minerals 12:1161. https://doi.org/10.3390/min12091161

SMEDA (2022) Small and Medium Enterprise Development Authority, District economic profile Lasbela.

Souri T, Watanabe M, Sakagami K (2006) Contribution of parker and product indexes to evaluate weathering condition of yellow brown forest soils in Japan. Geoderma 130:346–355. https://doi.org/10.1016/j.geoderma.2005.02.007

Sposito G (2008) The chemistry of soils, 2nd edn. Oxford University Press Inc, New York, p 329

Srikhumsuk P, Peshkur T, Renshaw JC, Knapp CW (2023) Toxicological response and bioaccumulation of strontium in *Festucarubra* L. (red fescue) and *Trifoliumpratense* L. (red clover) in contaminated soil microcosms. Environ Sys Res 12:15. https://doi.org/10.1186/s40068-023-00297-5

Sultana S, Khatun HA, Faruquee M, Islam MMU, Tonny HJ, Islam MR (2023) Comparison between acid digestion (ICP-OES) and X-ray fluorescence (XRF) spectrometry for zinc concentration determination in rice (*Oryza sativa* L.). Foods 12:1044. https://doi.org/10.3390/foods12051044

Syed NA, Siddiqa T, Sohoo N (2020) Evaluation of morphodynamics of MianiHor, a coastal lagoon of Lasbela, Balochistan, Pakistan. Oceanologia 62(1):45–55. https://doi.org/10.1016/j.oceano.2019.07.002

Tasrina RC, Rowshon A, Mustafizur AMR, Rafiqul I, Ali MP (2015) Heavy metals contamination in vegetables and its growing soil. J Environ Anal Chem 2:1–6. https://doi.org/10.4172/2380-2391.1000142

Tepanosyan G, Pipoyan D, Beglaryan M, Sahakyan L (2022) Compositional features of Pb in agricultural soils and geochemical associations conditioning Pb contents in plants. Chemosphere 306:135492. https://doi.org/10.1016/j.chemosphere.2022.135492

Tunçay T, DengizO BI, Kilic S, Baskan O (2019) Chemical weathering indices applied to soils developed on old lake sediments in a semi-arid region of Turkey. Eur J Soil Sci 8(1):60–72. https://doi.org/10.18393/ejss.499122

Wang Z, Tian H, Tan X, Wang F, Jia H, Megharaj M, He W (2019) Long-term As contamination alters soil enzyme functional stability in response to additional heat disturbance. Chemosphere 229:471–480. https://doi.org/10.1016/j.chemosphere.2019.05.055

Wani KI, Naeem M, Aftab T (2022) Chromium in plant-soil nexus: speciation, uptake, transport and sustainable remediation techniques. Environ Pollu 315:12035. https://doi.org/10.1016/j.envpol.2022.120350

Wei Y, Wang R, Zhang J, Guo H, Chen X (2023) Partition management of soil nutrients based on capacitive coupled contactless conductivity detection. Agriculture 13:313. https://doi.org/10.3390/agriculture13020313

Wu Q, Wan R, Li Q, Mo W, Liu J, Zhao C, Peng S (2022) Transformation of chromium speciation during high hexavalent chromium-contaminated soil remediation by CPS and biostimulation. Agronomy 12(4):801. https://doi.org/10.3390/agronomy12040801

Xu X, Shao L, Lan B, Wang S, Hilton J, Qin J, Hou H, Zhao J (2020) Continental chemical weathering during the Early cretaceous oceanic anoxic event (OAE1b): a case study from the Fuxin Fluvio-lacustrine basin, Liaoning Province, NE China. J Palaeogeo. https://doi.org/10.1186/s42501-020-00056-y

Yang S, He M, Zhi Y, Chang SX, Gu B, Liu X, Xu J (2019) An integrated analysis on source-exposure risk of heavy metals in agricultural soils near intense electronic waste recycling activities. Environ Int 133:105239. https://doi.org/10.1016/j.envint.2019.105239

Zhang T, Wang T, Wang W, Liu B, Li W, Liu Y (2020a) Reduction and stabilization of Cr (VI) in soil by using calcium polysulfide: Catalysis of natural iron oxides. Environ Res 190:109992. https://doi.org/10.1016/j.envres.2020.109992

Zhang W, Kang Z, Wang Q, Qiu N, Chen M, Zhou F (2020) The biological effects of strontium (88Sr) on Chinese cabbage. Plant Soil Environ 66(4):149–154. https://doi.org/10.17221/108/2020-PSE

Zhao Z, Jiang H, Kong L, Shen T, Zhang X, Gu S, Li Y (2021) Assessment of potential ecological risk of heavy metals in surface soils of Laizhou. Eastern China Water 13(21):2940. https://doi.org/10.3390/w13212940

Zulfiqar U, Farooq M, Hussain S, Maqsood M, Hussain M, Ishfaq M, Ahmad M, Anjum MZ (2019) Lead toxicity in plants: Impacts and remediation. J Environ Manag 250:109557. https://doi.org/10.1016/j.jenvman.2019.109557